# IPS Meeting 2012
# 23 - 24 February

Institute of Physics Singapore

# Conference Program

The IPS Meeting 2012 thanks its sponsors
for their generous support

iMath
Simplifying Complexity

Agilent Technologies

LASER21

tme
Partnership . Differentiation . Innovation

CQT Centre for Quantum Technologies

NUS National University of Singapore

# 1 Foreword

Dear fellow Physicists,

The IPS Meeting 2012 is another step in our exciting journey to make Singapore a place where premier physics research is carried out. And I'd like to take the opportunity to thank you all for getting together for this scientific interchange. Compared to last year's meeting, we tried to have a stronger focus on research – not to neglect our ties to the secondary education institutes, but to strengthen communication between researchers and to make sure that we are really internationally competitive in this area. While there are numerous meetings we all attend all the time, let's make sure that we form an identity as physicists here in Singapore, by having a strong annual research meeting of our own. The IPS Meeting is the ideal opportunity to find out what your colleague is doing – be it next doors, at another university or even another research institute.

We are particularly happy to see so many original poster contributions from many research groups this year. Make sure you spend ample time to look at them! Last year, we felt that this gives us an opportunity for much better communication. Thus, posters are located such that they are easy to find. To set the perfect environment to stop by, catch up with your colleagues and have an informal conversation about science, we will cater food and drinks during the poster sessison. And last but not least the three best poster presentations will be honored with the IPS Best Poster Award on Friday afternoon.

We also received many interesting submissions for contributed talks and had a particularly hard time deciding who to award the limited slots. Together with the invited talks, these contributions promise plenty of excitement during the sessions. One particularly hot research topic this year is Graphene, where both universities have carried out lots of nice work, that moved from basic research and exciting electronic properties to applications in an amazingly short time.

Let me also take the opportunity to thank the organizing committee for its effort in making this event happen. We had strong support from both NTU and NUS, with Zhang Qing coordinating the NTU effort, and Sow Chorng Haur on the NUS side, and also from Koh Wee Shing from ASTAR. Big thanks to logistics support from Lim Kim Yong, Andreas Dewanto, Alexander Ling, the physics society of NUS and staff of NUS Science faculty and the Centre for Quantum Technologies. In addition we'd like to the Institute of Advanced Studies for their support in organizing the poster sessions and the Faculty of Science for providing the conference venue. Again very special thanks go to Markus Baden, who managed all the details to ensure a clear composition of the scientific program. And of course we also like to say a big thank you to our exhibitors and sponsors for their generous support.

Christian Kurtsiefer, Chairman IPS Meeting 2012
Leong-Chuan Kwek, President of the Institute of Physics Singapore

# Contents

# 2 Schedule

### Thursday, February 23

| | | | |
|---|---|---|---|
| 8.00 AM | Registration | | |
| 8.50 AM | Opening Address, LT31 | | |
| 9.00 AM | Plenary Talk by Harald Fritzsch, LT31 | | |
| 9:45 AM | Plenary Talk by Serge Haroche, LT31 | | |
| 10.30 AM | Coffee/Tea Break + Exhibition | | |
| 11.00 AM | T2: Seminar Conductor Light Sources/ Econophysics LT31 | T3: Thin Films S16-03-07 | T4: THz Physics S16-03-04 |
| 12.30 PM | Lunch + Poster Session P1 + Exhibition | | |
| 2.00 PM | T5: Nanofabrication/ Graphene Electronics LT31 | T6: Quantum Physics S16-03-07 | |
| 3.30 PM | Coffee/Tea Break + Exhibition | | |
| 4.00 PM | T7: Graphene I LT31 | T8: Atomic & Optical Physics S16-03-07 | T9: Energy & Materials S16-03-04 |

**Friday, February 24**

| | | | |
|---|---|---|---|
| 9.00 AM | T10: Biophysics LT31 | T11: Optical Characterization of Condensed Matter S16-03-07 | T12: Semiconductors S16-03-04 |
| 10.30 AM | Coffee/Tea Break + Exhibition | | |
| 11.00 AM | T13: Graphene II LT31 | T14: Photonic Devices/ Astrophysics S16-03-07 | T15: Carbon Nanotube/ Physics of Continua S16-03-04 |
| 12.30 PM | Lunch + Poster Session P2 + Exhibition | | |
| 2.00 PM | T16: Novel Optical Materials LT31 | T17: Physics of Bubbles S16-03-07 | |
| 3.30 PM | IPS Poster Award Ceremony, LT31 | | |
| 3.45 PM | Coffee/Tea Break + Exhibition | | |
| 4.00 PM | T18 Metamaterials LT31 | T19: Nanoactuators S16-03-07 | T20: Organic Electronics |

# 3 Location Map

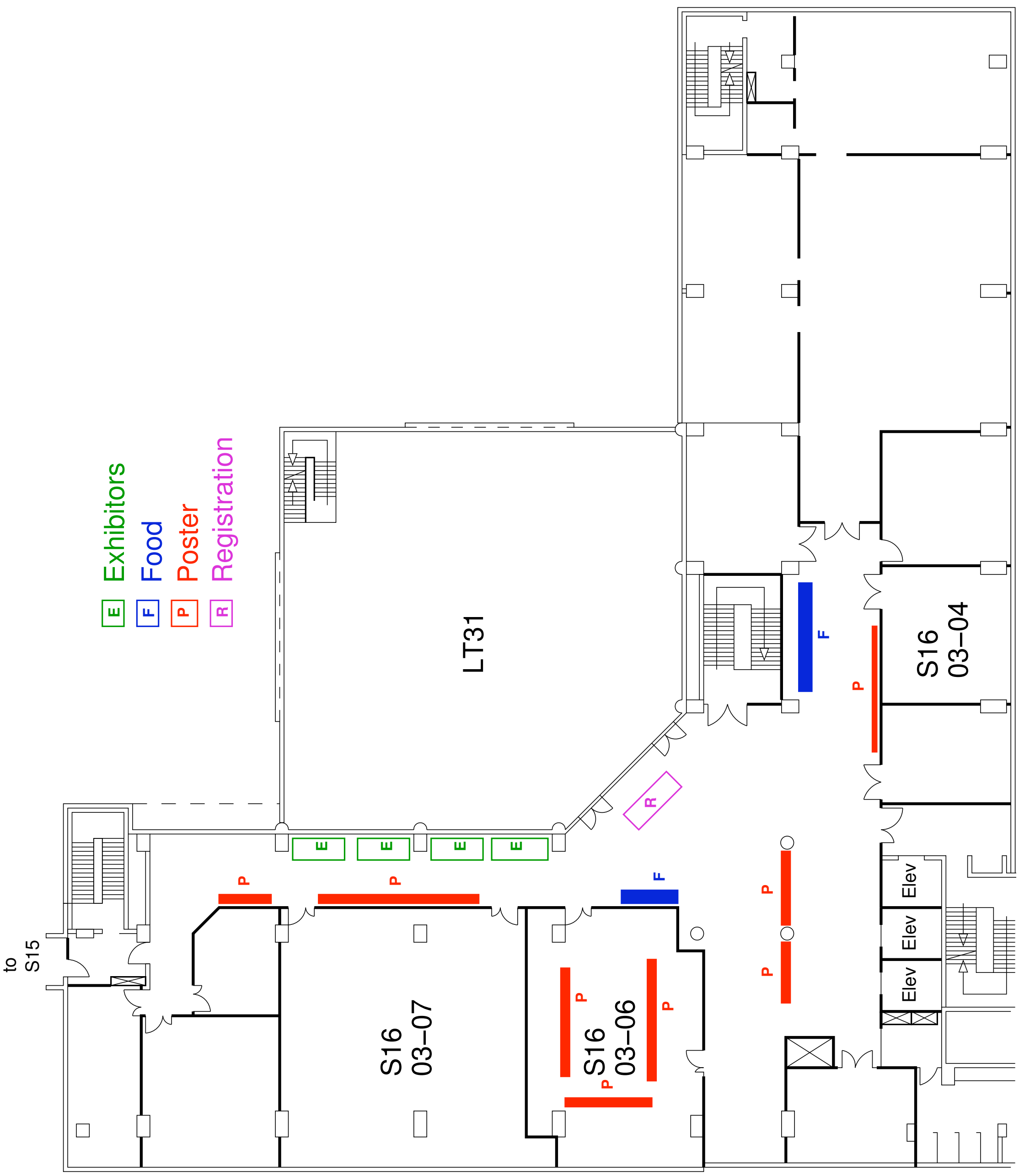

# 4 Plenary Session - Thursday

### Harald Fritzsch: From quarks to chromodynamics

Thursday, Februrary 23 - 9.00 AM Lecture Theatre LT 31

**Abstract**
Today QCD is regarded as the correct theory of the strong interactions. In 1971 Gell-Mann and I introduced the color quantum number of the quarks, one year later the exact color symmetry group was interpreted as the gauge group of QCD. The self-coupling of the gluons leads to the property of asymptotic freedom and to the confinement of the quarks and gluons. The proton mass can be calculated, but the quark masses are free parameters. The quarks and gluons have been observed at high energies as hadronic jets.

**About the speaker**
Professor Harald Fritzsch has made various contributions to Quantum Chromodynamics, to Grand Unified Theories and to the physics of quarks and leptons. Together with Murray Gell-Mann he has introduced the concept exact color symmetry which led to foundations of Quantum Chromodynamics.

During his career Professor Harald Fritzsch worked at the Stanford Linear Accelerator, CERN, the California Institute of Technology, the University of Wuppertal, the University of Berne and the Ludwig-Maximilians University of Munich, where he holds the chair of theoretical physics since 1980.

### Serge Haroche: Juggling with photons in a box to explore the quantum world

Thursday, Februrary 23 - 9.45 AM Lecture Theatre LT 31

**Abstract**
Atoms interacting with microwave photons trapped between highly reflecting superconducting mirrors realize an ideal system to perform some of the thought experiments imagined by the founding fathers of quantum physics and to illustrate fundamental aspects of measurement theory. The experiments performed with this system include the non-destructive counting of photons, the recording of field quantum jumps, the reconstruction of "Schrödinger cat" states of radiation and the study of their decoherence which provides a striking illustration of the transition from the quantum to the classical world. Juggling with non-classical photonic states has recently been extended by implementing quantum feedback methods. They fight decoherence by monitoring in real time the field quantum jumps before reversing their effects. The generalization of these studies to systems in which real atoms are replaced by artificial ones will be mentioned.

**About the speaker**
Professor Serge Haroche has made a series of experiments that transformed some of the oldest thought experiments of quantum mechanics into realities in the laboratory. His

contributions to the field of cavity quantum electrodynamics with Rydberg atoms and microwave cavities have led to a better understanding of fundamental quantum systems. Many of the techniques developed are now applied in a variety of different physical systems that can be described by the same set of tools.

Currently Professor Serge Haroche holds the chair of quantum physics at Collège de France, and his research takes place at the laboratoire Kastler Brossel at the Ecole Normale Supériore. During his career he worked at Paris VI University, Stanford University, Ecole Polytechnique, Harvard and Yale University and many others.

# 5 Posters

### IPS Best Poster Award

During the conference the program committee will select the three best poster presentations for the IPS Best Poster Award. The award will be handed over to the winners at the ceremony Friday 3.30 pm in the lecture theatre LT 31.

### Logistics

Posters are presented in two sessions. The first session will be held on Thursday, the second on Friday. Both sessions are from 12.30 pm to 2 pm. During the poster session there will be catered lunch for all participants of the conference.

All authors are kindly requested to put their poster up in the morning of the day of their session, and put them down by 4 pm that day. Each poster is assigned a panel which corresponds to the number after the dot in the number listed below, e.g., the panel no. 13 is reserved for P1.23 on the first and for P2.23 on the second day. The format of the poster will be A1 portrait.

## 5.1 P1 Poster Session 1 (Thursday)

### P1.1 Crosstalk calibration of Multi Pixel Photon Counters by measurement of the second-order intensity correlation function of coherent light.

Dmitry Kalashnikov, Si Hui Tan, Leonid Krivitskiy

Thursday 12.30 PM, Foyer/Hallway, Panel 1

We propose a new accessible method for calibration of crosstalk for Multi Pixel Photon Counters (MPPC). The one is based on the measurement of the normalized second order correlation function of coherent light and the generalized crosstalk model. The method was tested for several MPPCs with different pixel size and at different temperatures. The obtained results were compared with the ones obtained by the conventional dark count method for the same detectors under the same conditions. Two methods were found to be in good agreement qualitatively. However, the proposed method exhibits much less uncertainty in determination of the crosstalk in the case of low dark counts.

### P1.2 Efficient, Narrowband PPKTP Source for Polarization Entangled Photons

Siddarth Koduru Joshi, Chen Ming Chia, Felix Anger, Antia Lamas-Linares, Christian Kurtsiefer

Thursday 12.30 PM, Foyer/Hallway, Panel 2

The underlying protocols behind many applications often require a complete detection of almost all entangled photons to outperform their classical counterparts. While photodetectors have come close to unit detection efficiency (¿95current bottleneck in applications requiring a high efficiency. We present a high efficiency photon pair source which addresses this issue. A pump laser (lambda= 405 nm) is focused into a type II PPKTP crystal, where it undergoes spontaneous parametric down-conversion into signal and idler modes collinear with the pump mode, maximizing the mode overlap between the target modes. To obtain polarization entangled photons, we pump the crystal from both directions and interferometrically combine the two downconverted paths in a Sagnac interferometer. We experimentally optimized the focusing parameters for a maximal efficiency and we observe uncorrected efficiencies ¿ 35This efficiency is the value obtained from uncorrected count rates from Silicon Avalanche Photo Diodes (Si APDs) of 49.7±2photons. No corrections are applied. Our source efficiency ( 71[1] A.E. Lita, A.J. Miller, S.W. Nam,Opt. Express 16, 3032 (2008)

## P1.3 Anderson Localization of Dirac Fermions on a Honeycomb Lattice

Kean Loon Lee

Thursday 12.30 PM, Foyer/Hallway, Panel 3

We study the tight-binding model with uncorrelated diagonal disorder on a honeycomb lattice. We use three independent methods: recursive Green's function, self-consistent Born approximation and time-evolution of a Gaussian wave packet, to extract scattering mean free path $\ell$s, scattering mean free time $\tau$ , density of states $\rho$ and localization length $\xi$. The three methods give excellent quantitative agreement of the single-particle properties ($\ell$s, $\tau$, $\rho$). Furthermore, a finite-size analysis of $\xi$ reveals that the finite-size localization lengths of different lattices and different energies (including the charge neutrality point of a honeycomb lattice) can be described by the same single-parameter curve. However, the extracted numerical value of $\xi$ show great deviation from the prediction of self-consist theory of localization. The inadequacy of the self-consistent theory in this insulating phase is further revealed by the anomalous decrease in the averaged displacement of a wave packet after one $\tau$ .

## P1.4 Control and manipulation of cold molecular ions

Shiqian Ding, Meng Gao, Dzmitry Matsukevich

Thursday 12.30 PM, Foyer/Hallway, Panel 4

Due to their rich level structure, long trapping time and good isolation from the environment, molecular ions confined in the rf-Paul trap are attractive for precision measurements, spectroscopy and studies of the quantum mechanical aspects of chemical reactions. However, the preparation and detection of quantum states of molecular ions remains a difficult task. Here, we introduce a scheme to cool both the motional and internal states of the molecular ions. The molecular ion is sympathetically cooled to the ground state of motion via co-trapped atomic ions, while the molecular rovibrational states (internal states) are initialized with the help of optical pumping by broadband light and manipulated via stimulated Raman transition with a frequency comb. We also describe the associated quantum logic scheme to detect the state of the molecular ion. The progress towards its experimental implementation is presented as well.

## P1.5 Vibrational ground state cooling of a neutral atom in a tightly focused optical dipole trap.

Xu Heng Victor Leong, Kadir Durak, Syed Abdullah Aljunid, Gleb Maslennikov, Christian Kurtsiefer

Thursday 12.30 PM, Foyer/Hallway, Panel 5

Recent experiments have shown that an efficient interaction between a single trapped atom and light can be established by concentrating light field at the location of the atom by focusing [1-3]. However, to fully exploit the benefits of strong focusing one has to localize the atom at the maximum of the field strength [4]. The position uncertainty due to residual kinetic energy of the atom in the dipole trap (with a depth of approximately 1 mK) after molasses cooling is significant (few 100 nm). It limits the interaction between a focused light mode and an atom already or moderate focusing strength [2]. To address this problem we implement a Raman Sideband cooling technique, similar to the one commonly used in ion traps [5], to cool a single Rb atom to the ground state of the trap. We have cooled the atom along the transverse trap axis (trap frequency 55 kHz), to a mean vibrational state n=0.55 and investigate the impact on atom-light interfaces.

[1] M. K. Tey, et al., Nature Physics **4** 924 (2008) [2] M. K. Tey et. al., New J. Phys. **11**, 043011 (2009) [3] S.A. Aljunid et al., Phys. Rev. Lett. **103**, 153601 (2009) [4] C. Teo and V. Scarani Opt. Comm. **284** 4485-4490 (2011) [5] C. Monroe et al., Phys. Rev. Lett. **75**, 4011 (1995)

## P1.6 Challenges in Ultrafast Spectroscopy using Reflection Geometry

Ho Fai Leung, Michael Kurniawan, Tze Chien Sum

Thursday 12.30 PM, Foyer/Hallway, Panel 6

Transmission geometry transient absorption spectroscopy has been widely used to understand excitation dynamics of organic photovoltaics among other materials. However, transmission geometry would not be applicable for samples which comprise an opaque electrode layer, an example of which includes Field-Assisted Pump Probe Spectroscopy (FAPP). In such situations, reflection geometry is required. It has been found however, that this mode presents several challenges. For my Final Year Project, I aim to investigate the challenges faced when one does ultrafast spectroscopy in reflection geometry. The samples used comprise an Indium Tin Oxide (ITO) layer and a pure P3HT layer on top of it. Aluminium is then coated on top of the pure P3HT layer to act as the reflection boundary. The scope of this project is to understand how various sample parameters such as thickness affect the presence of unwanted optical effects in the differential reflection spectra, as well as other factors such as the effect of plasma treatment. Ultimately, I hope to be able to produce a concrete method for the preparation of a sample which can be used confidently for more advanced experiments such as FAPP.

## P1.7 Narrowband Source of Correlated Photon Pairs via Four-Wave Mixing in Atomic Vapour

Bharath Srivathsan, Gurpreet Kaur Gulati, Mei Yuen Brenda Chng, Gleb Maslennikov, Dzmitry Matsukevich, Christian Kurtsiefer

Thursday 12.30 PM, Foyer/Hallway, Panel 7

Many quantum communication protocols require entangled states of distant qubits which can be implemented using photons. To efficiently transfer entanglement from photons to stationary qubits such as atoms, one requires entangled photons with a frequency bandwidth matching the absorption profile of the atoms. In our setup, a cold Rb 87 atomic ensemble is pumped by two laser beams (780nm and 776nm) resonant with the 5S-1/2 -¿ 5P-3/2 -¿ 5D-3/2 transition. This generates time-correlated photon pairs (776nm and 795nm) by non-degenerate four-wave mixing via the decay path 5D-3/2 -¿ 5P-1/2 -¿ 5S-1/2. Coupling the photon pairs into single mode fibers and using silicon APDs, we observe g(2) of about 2000 and pairs to singles ratio of 11.2

## P1.8 Transmittance Spectrum and Coupling of Surface Plasmon Resonances in a Gold Gratings System: A Simulation Study

Wei Peng Goh, Wee Shing Koh, Joel K. W. Yang

Thursday 12.30 PM, Foyer/Hallway, Panel 8

The transmittance spectrum of a gold grating system and its accompanying surface plasmon resonances (SPRs) are studied. A double grating structure is conceived such that both sets of gratings are fabricated on top of each other. The advantage of having such a structure is the absence of a lift-off during fabrication. Upon excitation at the resonance frequency, coupling is observed between the metallic strips as well as between both sets of grating system. This stacking configuration enables plasmon excitation over a larger excitation volume. Through simulation studies, we can able to determine the SPRs by plotting the transmittance spectra. The periodicity, line width and height (between both sets of gratings) can be varied so that the SPRs can be tuned appropriately. Possible applications of the grating system include solar cells and biosensors.

## P1.9 Accuracy of Second Order Perturbation theory in the Polaron and Variational Polaron Frames

Chee Kong Lee, Jeremy Moix, Jianshu Cao

Thursday 12.30 PM, Foyer/Hallway, Panel 9

In the study of open quantum systems, the polaron transformation has recently attracted a renewed interest as it offers the possibility to explore the strong system-bath coupling regime. Despite this interest, a clear and unambiguous analysis of the regimes of validity of the polaron transformation is still lacking. Here we provide such a benchmark, comparing second order perturbation theory results in the original untransformed frame, the polaron frame and the variational extension with numerically exact path integral calculations of the equilibrium reduced density matrix. Equilibrium quantities allow a direct comparison of the three methods without invoking any further approximations as is usually required in deriving master equations. It is found that the second order results in the original frame are accurate for weak system-bath coupling, the full polaron results are accurate in the opposite regime of strong coupling, and the variational method is capable of interpolating between these two extremes. As the bath becomes more non-Markovian (slow bath), all three approaches become less accurate.

## P1.10 All-optical AND and OR logic gates in a plasmonic racetrack resonator structure

Peiwen Wang, Bin Hu, Qijie Wang

Thursday 12.30 PM, Foyer/Hallway, Panel 10

All-optical AND and OR logic gates using a subwavelength plasmonic racetrack resonator embedded with nonlinear optical Kerr medium are proposed and numerically demonstrated. Due to the confinement of surface plasmons, the logic gate is as small as 1.5µm×1.4µm. The transmission of one port of the structure can be modulated by the input intensities through optical Kerr effect. Therefore, two input optical signals representing the two operands are applied to one port of the racetrack resonator simultaneously in order to realize the logic operations. The finite-difference time-domain simulations manifest that AND and OR operations can be realized at a wavelength of 1.55µm by defining different light intensities as ‘1’ and ‘0’.

## P1.11 Generation of nonclassical light in waveguide arrays

Amit Rai, Dimitris Angelakis

Thursday 12.30 PM, Foyer/Hallway, Panel 11

We study a class of waveguide arrays where the waveguides contain second order nonlinearity and are coupled through the evanescent overlap of the guided modes. As a relevant application, we investigate the viability of such an array as a platform for studying the continuous variable information processing in an integrated manner. In particular, we explore the possibility of generating broadband continuous variable entanglement in an integrated manner on the waveguide chip without the use of bulk optical elements. Our system allows continuous variable entanglement to be generated between spatially separated modes that are coupled through the evanescent overlap of the guided modes. The entanglement generated between the spatially separated waveguide modes can be experimentally measured by using the homodyne detectors scanning across the waveguide array output. We also address the effect of loss on entanglement dynamics of waveguide modes and show that the waveguide structures are reasonably robust against the effect of loss.

## P1.12 Investigation of Dielectric Loaded Surface Plasmon Waveguide Structures by Using Transfer Matrix Method

Xiaoyong He, Qijie Wang

Thursday 12.30 PM, Foyer/Hallway, Panel 12

Dielectric loaded surface plasmon polariton (DLSPP) waveguide is formed by a dielectric stripe deposited on a metal surface, showing the merits of strong lateral confinement and low losses. The propagation properties of DLSPP waveguide structures have been investigated by using transfer matrix method (TMM). By taking the Full Width Half Maximum of the optical mode as the effective optical mode width in the numerical calculations, the results obtained from the TMM agree well with those from finite element method (FEM). Compared to the FEM and FDTD methods, the TMM has the advantages of simplicity and high efficiency. As a demonstration, we investigate the waveguide properties of DLSPPs structures in the terahertz and near-infrared regimes. The results may find many important applications in integrated photonic devices and sensors.

## P1.13 Collective Scattering and Cooling in Cavity Quantum Electrodynamics

Kyle Arnold, Markus Baden, Murray Barrett

Thursday 12.30 PM, Foyer/Hallway, Panel 13

We report our progress in the study of collective scattering effects with ultracold atoms coupled to a high-finesse optical resonator. In order to observe collective scattering from the side into the resonator, we trap up to 10'000 rubidium atoms in a deep two-dimensional optical lattice with a lattice spacing of the wavelength of the scattered light. In this setup, all atoms are coupled identically to the resonator and light scat- tered into the resonator by individual atoms interferes constructively. In addition, high trapping frequencies with respect to the resonator linewidth allow us to study cavity cooling.

## P1.14 Observing neutrino oscillations with trapped ions

Changsuk Noh, Blas Rodriguez-Lara, Dimitris Angelakis

Thursday 12.30 PM, Foyer/Hallway, Panel 14

We propose a scheme to observe the dynamics of neutrino oscillations using trapped ions. For neutrinos in 1+1 dimensions, our scheme is experimentally implementable with existing trapped ion technology. We show that the three generation neutrino oscillations can be realized with three ions for 1+3 and 1+1 dimensions where the latter case only requires experimentally proven two-ion interactions. For this case, we discuss two setups utilizing different types of spin- spin interactions. Our method can be readily applied to two generation neutrino oscillations requiring fewer ions and lasers. We give a brief outline of a possible experimental scenario.

## P1.15 Probing the BCS-BEC crossover with photons in a nonlinear optical fiber

Mingxia Huo, Changsuk Noh, Blas Rodriguez-Lara, Dimitris Angelakis

Thursday 12.30 PM, Foyer/Hallway, Panel 15

We propose a scheme where photons generated inside a nonlinear optical fiber can mimick and analyze the crossover from weakly to strongly bound fermionic pairs as predicted by the BCS theory in one dimension. We first show how stationary light-matter excitations (polaritons) in the system can realize an optically tunable two-component Bose-Hubbard model. We then analyze the optical parameters regime necessary to generate an effective Fermi-Hubbard model of polaritons exhibiting the equivalent of Cooper pairing in one dimension. The predicted behaviour characterized by a crossover from short- to long-range spatial correlations as interactions are tuned, can be efficiently observed for all parameter regimes utilizing the in situ accessibility of coherence functions of the light exiting the fiber.

## P1.16 A Luttinger liquid of photons and spin-charge separation in hollow-core waveguides

Dimitris G Angelakis, Ming-Xia Huo, Elica Kyoseva, Leong Chuan Kwek

Thursday 12.30 PM, Foyer/Hallway, Panel 16

In this work we show that light-matter excitations (polaritons) generated inside a hollow one-dimensional fiber filled with two types of atoms, can exhibit Luttinger liquid behaviour. We explain how to prepare and drive this quantum-optical system to a strongly interacting regime, described by a bosonic two-component Lieb Lininger model. Utilizing the connection between strongly interacting bosonic and fermionic systems, we show how spin-charge separation could be observed by probing the correlations in the polaritons. This is performed by rst mapping the polaritons to propagating photon pulses and then measuring the eective photonic spin and charge densities and velocities by analyzing the correlations in the emitted photon spectrum. The necessary regime of interactions is achievable with current quantum optical technology.

## P1.17 Pinning quantum phase transition of photons in a hollow-core fiber

Ming-Xia Huo, Dimitris G Angelakis

Thursday 12.30 PM, Foyer/Hallway, Panel 17

We show that a pinning quantum phase transition for photons could be observed in a hollow-core one-dimensional fiber loaded with a cold atomic gas. Utilizing the strong light confinement in the fiber, a range of different strongly correlated polaritonic and photonic states, corresponding to both strong and weak interactions can be created and probed. The key ingredient is the creation of a tunable effective lattice potential acting on the interacting polaritonic gas which is possible by slightly modulating the atomic density. We analyze the relevant phase diagram corresponding to the realizable Bose- Hubbard (weak) and sine-Gordon (strong) interacting regimes and conclude by describing the measurement process. The latter consists of mapping the stationary excitations to propagating light pulses whose correlations can be e±ciently probed once they exit the fiber using available optical technologies.

## P1.18 Ultrafast Laser Spectroscopy of Rubrene

Lin Ma, Keke Zhang, Christian Kloc, Gagik Gurzadyan

Thursday 12.30 PM, Foyer/Hallway, Panel 18

Excited state dynamics of rubrene in solution and single crystal were studied by femtosecond pump-probe and time-resolved fluorescence spectroscopy under various excitation conditions. Singlet fission is proven to play a dominated role during the excited state relaxation of rubrene single crystal. Since by consumption of one singlet exciton, two triplet excitons are generated, singlet fission is considered to hold the potential to improve the efficiency of optoelectronics or photovoltaics. Under 500 nm excitation, triplet excitons are formed in the time scale of 2 and 20 ps in rubrene single crystal, which is explained by thermally activated singlet fission from lowest vibrational state of the first excited singlet state S1. Under 250 nm excitation, 200 fs direct singlet fission from the upper excited singlet states SN is observed. Moreover, polarons are clarified to be directly generated from hot upper excited singlet states.

## P1.19 Simulating interacting relativistic theories with photons in hollow-core waveguides

Dimitris G Angelakis, Ming-Xia Huo, Darrick Chang, Leong Chuan Kwek, Vladimir Korepin

Thursday 12.30 PM, Foyer/Hallway, Panel 19

Photonic quantum simulations of one dimensional many-body systems have attracted renewed interest lately with works on photon crystallization and Luttinger liquids. In this work we show that the quantum Thirring model for interacting fermions in (1+1) dimensions can be realized using stationary polaritons in hollow-core waveguides loaded with atoms. By controlling optical parameters such as one-photon detunings and external laser intensities, the massless and the massive Thirring models are realizable. Coherently mapping the polaritons into propagating photons allows for the direct probing of the relevant correlation functions and scaling behaviours characteristic of the underlying theories in question.

## P1.20 Experimental Realization of an Approximate Partial Transpose for Photonic Two-Qubit Systems

Hyang-Tag Lim, Yong-Su Kim, Young-Sik Ra, Joonwoo Bae, Yoon-Ho Kim

Thursday 12.30 PM, Foyer/Hallway, Panel 20

We report the first experimental realization of an approximate partial transpose for photonic two-qubit systems. The proposed scheme is based on the local operation on single copies of quantum states and classical communication, and therefore can be easily applied for other quantum information tasks within current technologies. Direct detection of entanglement, i.e., without performing quantum state tomog- raphy, using the partial transpose operation, is also demonstrated.

## P1.21 Probing Planck Time

Peng Kian Tan, Yen Chin Ong

Thursday 12.30 PM, Foyer/Hallway, Panel 21

Planckian structures such as Planck Time which is approximately 5.4 x 10^-44 second and Planck Length which is approximately 1.6 x 10^-35 metre are too small for Earth-bound experiments to resolve. We attempt to navigate around this constraint by measuring astronomical light sources.

Temporal intensity interferometric measurements of distant objects might be able to reveal an effect due to an accumulation of phase uncertainty in photons over time, which in turn will provide experimental evidence for Planck Time and its observable upper bound, and for or against various quantum gravity models.

## P1.22 Radiation Analysis for Low Earth Orbit Satellites

Alexander Ling, Rakhitha Chandrasekara, Yue Chuan Tan, William Morong

Thursday 12.30 PM, Foyer/Hallway, Panel 22

We are developing a small physics package (fitted to a small satellite), capable of performing Bell's inequality test in Low Earth Orbit(LEO). Radiation analysis is a crucial stage in the development cycle of a satellite application. This allows us to estimate how our micro and opto-electronic circuits would work in a specific satellite trajectory. We are interested in Total ionizing Dose(TID) which is a measure of exposure to radiation. Our physics package should be able to withstand the radiation in space for at least 2-3 months. In order to estimate the radiation dosage on our system we have used the online simulation software known as SPENVIS which is provided by the European Space Agency(ESA). In this paper, we present some results from this simulation software.

## P1.23 Towards 6Li-40K dipolar ground state molecules

Johannes Gambari, Kanhaiya Pandey, Mark Lam

Thursday 12.30 PM, Foyer/Hallway, Panel 23

With the coherent transfer of Feshbach molecules, created in highly excited vibrational states, to the absolute singlet ro-vibrational ground state, a long standing scientific goal has been achieved [1-4]. Heteronuclear molecules like 6Li-40K in its absolute ground state possess a relatively large electric dipole moment. In a high phase space density, ultracold heteronuclear molecular samples are promising tools for quantum simulation of a large class of many-body effects as well as for quantum computation due to their long range anisotropic dipolar interactions.

In our group, work towards ground state transfer of the previously presented bosonic 6Li-40K Feshbach molecules [5] has been started, and currently a laser system for STIRAP (Stimulated Raman Adiabatic Passage) being built. The wavelengths required for the Raman laser system are 766nm and 522nm [6, 7], which are roughly 250nm apart. Since the transition strengths are low, pulse sequences need to be comparatively long. The high coherence times will be achieved by locking the frequency comb to the 767nm laser and the 522nm laser to the frequency comb. A high finesse cavity is used to narrow the 767nm laser to sub kHz linewidth using the Pound Drever Hall technique.

## P1.24 Realizing the Multiparticle Hanbury Brown–Twiss Interferometer Using Nitrogen-Vacancy Centers in Diamond Crystals

Li Dai, Leong Chuan Kwek

Thursday 12.30 PM, Foyer/Hallway, Panel 24

We demonstrate that the multiparticle Hanbury Brown–Twiss interferometer can be realized in a network of nitrogen-vacancy centers: for an N-particle system, the interference effect is manifested only in the Nth-order intensity correlation function. The interference effect can be enhanced through a postselection process in which the multipartite Greenberger-Horne-Zeilinger entanglement is generated and tested with Svetlichny inequality.

## P1.25 Bias Voltage Adjustment of Avalanche Photo Diode Using Window Comparator For Temperature Fluctuations

Yue Chuan Tan, Subash Sachidananda, Alexander Ling

Thursday 12.30 PM, Foyer/Hallway, Panel 25

This paper presents a dynamic and reliable method to control the bias voltage of APD under constant change of temperature by means of window comparator mechanism with a micro-controller.

## P1.26 Enhancing photocurrent transient spectroscopy by electromagnetic modeling

Majid Panahandeh-Fard, Zilong Wang, Eng Aik Chan, Heinrich Diesinger, Cesare Soci

Thursday 12.30 PM, Foyer/Hallway, Panel 26

Photoconductive switches are widely used for characterizing charge carrier dynamics in unknown semiconductors by photocurrent transient spectroscopy and for generation of picosecond electrical pulses and terahertz radiation. Both applications critically depend on the performance of the waveguide structure. Width and shape of the photocurrent transient depend on both the photoconductive material and the geometry of the switch. The shape of the observed pulse is deteriorated with respect to the intrinsic response of the active material because it is the convolution of the material response with the response of the waveguide architecture. Photoconductive gaps in coplanar lines generally perform better than gaps in microstrip lines due to the smaller line spacing and negligible dispersion over a wider frequency range. The drawback of coplanar switches is the incompatibility of lithographic steps with some materials such as organic semiconductors. A compromise seen in some studies is a microstrip gap that can be conveniently deposited without lithography, featuring transition to coplanar accesses. In this work we analyze different switch architectures by electromagnetic modeling, applying a new approach representing the switch as 4 port S-matrix. This modeling shows that switches with coplanar access improve the frequency response by an order of magnitude over the plain microstrip design, in agreement with experimental results. This proves the potential of the model in designing optimized switch structures, and in enhancing the accuracy of material response measurements by deconvolving the modeled structural response from the observed transients.

## P1.27 Search for Cosmic Strings in the COSMOS Survey

Ivan Teng

Thursday 12.30 PM, Foyer/Hallway, Panel 27

Cosmic strings are hypothetical linear topological defects, thought to be associated with phase transitions occurring during the very early formation of the Universe. Several cosmological models predict their existence and their discovery may help to explain the presence of some as yet observed but unexplained large- scale structure that has been observed. However, none has been observed.

The emergence of high-resolution wide-field astronomical surveys such as COSMOS has further stoked interest in the observation of cosmic strings. This is due to the challenge of detecting smaller mass cosmic strings over a larger fraction of the sky out to higher redshifts.

New techniques pertaining the detection methodology that are formulated for the search of cosmic strings in the COSMOS survey as well as tighter limits regarding cosmic string parameters that have also been established through the analytical pipeline shall be discussed in this poster presentation.

## P1.28 Investigating artificial gauge fields by ultracold fermionic Sr atoms

Tao Yang, Pramod Mysore Srinivas, Elnur Hajiyev, Zhong Yi Chia, Chang Chi Kwong, Frederic Leroux, David Wilkowski

Thursday 12.30 PM, Foyer/Hallway, Panel 28

In this experimental project, artificial gauge fields acting on a cold fermionic Strontium gas will be produced and investigated. A coherent nuclear spin superposition will attempt to be obtained by using a coherent two-photon coupling. The idea will be to store light in a coherent spin superposition in the form of a dark-state polarization then measure the storage time. The purely nuclear magnetic dipole moment of the Strontium ground state will allow us to imprint a spin structure with a long coherence time. Since the spin is nuclear, we expect that its coherence will be preserved in the presence of collision and gets long storage time. Preparation and detection of the nuclear spin components will be performed using optical transitions resonant with the long-lived 3P states. In the experiment, a 2D MOT after the Zeeman slower will be used to increase the brightness of the beam and filters out atoms which could not be cooled down and irrelevant isotopes. The ultracold gas will be produced using a magneto-optical trap on the narrow intercombinaison line follow by an evaporation ramp in a diople trap.

## P1.29 Soft x-ray emission studies in neon operated fast miniature plasma focus device

S. M. P. Kalaiselvi, Rajdeep Singh Rawat, Tan Tuck Lee Augustine, Alireza Talebitaher, Lee Choon Keat Paul

Thursday 12.30 PM, Foyer/Hallway, Panel 29

A dense plasma focus device is a device which can generate short lived plasma through electromagnetic compression and acceleration. The compressed pinch plasma column is so hot and dense that results in the emission of X-rays over wide energy range. Soft X-rays has potential and novel applications in the field of lithography, microscopy etc., hence it is worthwhile, making study on the emission of soft X-rays from this portable sub-kilo joules energy range fast miniature plasma focus device which due to lower energy storage can be operated at higher repetition rate. Given that, the miniature plasma focus device produce essentially the similar plasma characteristics as the large plasma focus device and that the machine parameters has been in the past tuned for optimal operation of this device in deuterium gas for neutron emission, this paper presents the optimization of miniature plasma focus device for neon gas operation for soft x-ray emission in single shot mode. New anode dimensions have been simulated using Lee Model code for construction of electrode assembly for neon gas operation and the influence of different pressure of the neon as working gas on the emission of soft X-rays is investigated. There are also future plans to make study on the other influential parameters and thereby optimize the device for efficient neon soft X-ray emission.

## P1.30 The Influence of different numbers of laser pulses on FePt thin films

Ying Wang, Rajdeep Singh Rawat, Usman Ilyas, Paul Lee, Tuck Lee Tan, Raju Vijayaraghavan Ramanujan, Fengji Li, Sam Zhang

Thursday 12.30 PM, Foyer/Hallway, Panel 30

Small nonoparticles with hard coercivity are highly desired by the magnetic data storage applications to achieve high areal density. The lowering of phase transition temperature is one of the most important ways to achieve small sized nanoparticles in hard magnetic phase. Here, different numbers of pre-annealing pulsed laser exposure shots were tried to achieve the phase transition of FePt nano-particles from chemically disordered A1 phase to chemically ordered L10 phase at a lower thermal annealing temperature. The influence of different number of pulsed laser exposures on the magnatic properties, crystal structures, topographies, and elemental composition of FePt thin films were studied and will be reported.

## P1.31 Entanglement and Discord in Spin Glass

Chee Yeong Koh, Leong Chuan Kwek

Thursday 12.30 PM, Foyer/Hallway, Panel 31

We study the entanglement and discord in spin glass. By using the Edwards-Anderson XX model, we consider the Hamiltonian for 3 and 4 particles for nearest neighbor and next nearest neighbor interactions and to solve for the entanglement through concurrence. A conjecture for the average concurrence was made by comparing the 3- and 4-particle case. With a fixed mean and changing variances for the coupling J, the concurrence and discord are numerically plotted against the temperature. For $J = 1$, the critical temperature is found to be 2.106. The entanglement was found to increase beyond the critical temperature as the variance increases. The spin-spin correlation for 3 particles is plotted as a function of temperature T.

### P1.32 Coherent cavity networks with complete connectivity

Elica Kyoseva, Almut Beige, Leong Chuan Kwek

Thursday 12.30 PM, Foyer/Hallway, Panel 32

When cavity photons couple to an optical fiber with a continuum of modes, they usually leak out within a finite amount of time. However, if the fiber is about 1 m long and linked to a mirror, photons bounce back and forth within the fiber on a much faster time scale. As a result, dynamical decoupling prevents the cavity photons from entering the fiber. In this paper, we use the simultaneous dynamical decoupling of a large number of distant cavities from the fiber modes of linear optics networks to mediate effective cavity-cavity interactions in a large variety of configurations. Coherent cavity networks with complete connectivity can be created with potential applications in quantum computing and in the simulation of the complex interaction Hamiltonians of biological systems.

## 5.2 P2 Poster Session 2 (Friday)

### P2.1 Zone-selective scoping (ZPS) of bonds & electrons at the atomic scale

Yanguang Nie, Chang Q Sun

Friday 12.30 PM, Foyer/Hallway, Panel 1

ZPS revealed the strong relaxation, localization, polarization and quantum entrapment associated with the undercoordinated atoms associated with surface, defects, and adatoms and clarified that Rh and Pt adatoms serve, respectively, as acceptor- and donor-like catalysts and that the Dirac-Fermion polarons originate from nonbonding electron polarization by the locally entrapped core charge.

1 Sun CQ, Atomic scale purification of electron spectroscopic information (USA patent Application No.: 2010/000230). 2010: USA. 2 Nie YG, Pan JS, Zheng WT, Zhou J, and Sun CQ, Atomic Scale Purification of Re Surface Kink States with and without Oxygen Chemisorption. J Chem Phys C, 2011; 115: 7450-7455. 3 Nie YG, Zhang X, Ma SZ, Wang Y, Pan JS, and Sun CQ, XPS revelation of tungsten edges as a potential donor-type catalyst. PCCP, 2011; 13: 12640-12645.

### P2.2 CuPd and AgPd interface quantum entrapment and polarization

Yanguang Nie, Chang Q Sun

Friday 12.30 PM, Foyer/Hallway, Panel 2

XPS and UPS revealed that CuPd and AgPd serve as, respectively, acceptor- and donor-like catalyst because of the heterocoordination-induced quantum entrapment and polarization in their valence and core bands.

1 Sun CQ, Wang Y, Nie YG, Mehta BR, Khanuja M, Shivaprasad SM, Sun Y, Pan JS, Pan LK, and Sun Z, Interface quantum trap depression and charge polarization in the CuPd and AgPd bimetallic alloy catalysts. Phys Chem Chem Phys, 2010; 12: 3131 - 3135 2. Sun CQ, Dominance of broken bonds and nonbonding electrons at the nanoscale. Nanoscale, 2010; 2: 1930-1961. 3.

## P2.3 ZnO meso-mechano-thermo bonding and electronic dynamics

Shouzhi Ma, Chang Q Sun

Friday 12.30 PM, Foyer/Hallway, Panel 3

From the perspectives of bond order-length-strength (BOLS) correlation and nonbonding electron polarization (NEP), we have correlated the elasticity, band gap, phonon frequency, thermal stability, dilute magnetism, hydrophobicity, and the enhanced catalytic ability of ZnO with formulation of their pressure, size, and temperature dependence using the local-bond averaging (LBA) approach. The measurable quantities are functionally correlated to the order, nature, length, and energy of the representative bond of the entire specimen and their responses to the applied stimuli. Bond order loss causes the remaining bonds between the under-coordinated atom to contract spontaneously associated with bond strength gain and the interatomic trapping potential well depression. Therefore, the increase of the single bond energy, reduction of atomic cohesive energy, localized densification of charge, energy, and mass occurring to the surface of skin depth dominate the property change of ZnO nanostructures as a function of size. Consequently, the increase of energy density augments the Young's modulus; the increase of the single bond energy enhances the Hamiltonian that determines Stokes shift and band gap expansion; the drop of atomic cohesive energy lowers the critical temperatures for melting and nucleation growth; the BOLS effect dictates the change of phonon dynamics; the polarization of the unpaired electrons by the densely-and-locally entrapped core charges originates the dilute magnetism, superhydrophobicity and the enhanced catalytic ability. Varying pressure and temperature also alters the bond length and energy and hence the physical properties of ZnO in a predictable way.

1 Sun CQ, Dominance of broken bonds and nonbonding electrons at the nanoscale. Nanoscale, 2010; 2: 1930-1961. 2 Tay YY, Li S, Sun CQ, and Chen P, Size dependence of Zn 2p 3/2 binding energy in nanocrystalline ZnO. Appl. Phys. Lett., 2006; 88: 173118. 3 Liu XJ, Li JW, Zhou ZF, Yang LW, Ma ZS, Xie GF, Pan Y, and Sun CQ, Size-induced elastic stiffening of ZnO nanostructures: Skin-depth energy pinning. Appl. Phys. Lett., 2009; 94: 131902. 4 Li JW, Yang LW, Zhou ZF, Liu XJ, Xie GF, Pan Y, and Sun CQ, Mechanically Stiffened and Thermally Softened Raman Modes of ZnO Crystal. J. Phys. Chem. B, 2010; 114: 1648-1651.

## P2.4 Electrospun Rice Grain-shaped TiO2 and Its CNT Composite as Stable Performance Anode Material for Rechargeable Li Ion Batteries

Peining Zhu, Yongzhi Wu, M. V. Reddy, A. Sreekumaran Nair, B. V. R. Chowdari, Seeram Ramakrishna

Friday 12.30 PM, Foyer/Hallway, Panel 4

Nanofiber- and rice grain-shaped TiO2 nanostructures and their composites with functionalized multiwalled carbon nanotubes were fabricated by electrospinning and subsequent sintering process for applications in Lithium ion batteries. The fabricated nanostructures were characterized by X-ray diffraction, Raman spectroscopy, X-ray photoelectron spectroscopy, scanning- and transmission electron microscopy and surface area measurements. All nanostructured materials showed average discharge-charge plateaux of 1.75 to 1.95V. The nanofibrous- and rice grain-shaped TiO2 nanomaterials showed stable performances of 136 mAh g-1 and 140 mAh g-1, respectively, till the end of 800 cycles in the cycling range of 1.0-2.8 V vs. Li at a current rate of 150 mA g-1. CNTs/ TiO2 (4 wt.

## P2.5 Effect of Molten Salt, Temperature on the Preparation and Electrochemical Studies of Co3O4

Zhang Beichen, M.V. Reddy Reddy

Friday 12.30 PM, Foyer/Hallway, Panel 5

Effect of Molten Salt, Temperature on the Preparation and Electrochemical Studies of Co3O4 Zhang Beichen a,b, M.V.Reddyb* , K.P. Lohc, B. V. R. Chowdarib a Dunman High School, 10 Tanjong Rhu Road, Singapore 436895 b Department of Physics, Solid State Ionics/advanced batteries lab/Graphene center, National University of Singapore, Singapore 117542 c Department of Chemistry, Graphene center, National University of Singapore, Singapore 117542 Corresponding author : phymvvr@nus.edu.sg Abstract Commercial lithium ion batteries uses graphite as an anode but this has low theoretical capacity (372 mAh/g), low volumetric density and forms dendrites readily with lithium. As a potential alternative for graphite, Co3O4 has a high theoretical capacity (890mAh/g) and low fading rate. Previously authors studied preliminary studies on electrochemical studies of Co3O4 prepared by Molten Salt Method(MSM) at LiNO3:LiCl at 280°C. Compared to other methods MSM has shown very favourable electrochemical performances. Thus, to explore the optimal preparation condition for Co3O4 using different temperature and molten salt like LiNO3:KNO3, NaNo3:KNO3, LiNO3:LiOH, KCl and studied its electrochemical properties, eleven differnt samples were prepared using different temperatures from 180OC to 710OC and different Co-salts such as Co-sulphate, Co- acetate and Co-hydroxide. The obtained Co3O4 powders were characterized X-ray diffraction, Rietveld refinement method, scanning electron microscopy (SEM), density and BET surface area methods. Anodic properties were evaluated by cyclic voltammetry and galvanostatic cycling. Galavanostatic cycling studies of Co3O4 using different Co-salts shows a reversible capacity values of 800 to 1050 mAh/g at current rate of 60 mA/g (0.065 C rate), the end of 40th cycle. Comparing across $Co_3O_4$ prepared in different temperature, $Co_3O_4$ prepared under 510oC shows a best capacity and sustainability; comparing $Co_3O_4$ prepared from different Cobalt source, $Co_3O_4$ from Co-hydroxide deliver highest and most stable capacity with the smallest capacity fading. The results also suggest a repeatable interesting trend for certain samples that the capacity increases during the cycling. The analysis of the reaction mechanism and the patterns of electrochemical performance of $Co_3O_4$ are discussed based on based CV and cycling results.

## P2.6 Charge Transfer Mechanisms of Metal Oxides and Modelling through Impedance Spectroscopy

Lim Yong Hui, Marcus Ng Kai Jie, Xu Hong Yun

Friday 12.30 PM, Foyer/Hallway, Panel 6

The aim of this project is to model the charge transfer mechanisms of magnesium doped lithium cobalt oxide ($LiCo_{0.97}Mg_{0.03}O_2$) and lithium cobalt oxide ($LiCoO_2$) and to find out the variation of basic physical parameters like resistance, capacitance and Li-diffusion co-efficient of $LiCo_{0.97}Mg_{0.03}O_2$ and lithium cobalt oxide ($LiCoO_2$). It was hypothesized that $LiCo_{0.97}Mg_{0.03}O_2$ is better based on impedance values. The coin cell was prepared using $LiCo_{0.97}Mg_{0.03}O_2$, and then subjected to Electrochemical Impedance Spectroscopy (EIS) and Galvanostatic Intermittent Titration Technique (GITT). Experimental Nyquist plots are modeled with equivalent electrical circuits by the combination of different resistors, capacitors and Warburg elements modeled through the Z-view software. In our project, we used several models, such as the Nobili, Bhonke model but it was found out that our own model was the most accurate and thus the most suitable to understand the charge transfer mechanisms. The GITT results were used to calculate the diffusion rate of lithium ions. The results were then analyzed and compared. It was found that $LiCo_{0.97}Mg_{0.03}O_2$ was a better choice to be used in lithium-ion coin cells, as it had higher lithium ion mobility as shown by the GITT results. Ion mobility refers to the ability for ions to move through a medium in response to an electric field.

## P2.7 Preparation of CuO and its high energy storage performance as anode material for lithium Batteries

Jiahuan Fan, Cai Yu, M V Reddy

Friday 12.30 PM, Foyer/Hallway, Panel 7

In this project, we reported the novel preparation of simple binary oxide, CuO by molten salt method at a temperature range of 280°C to 950°C for 3 hours in air.

Preparation of CuO and its high energy storage performance as anode material for lithium Batteries

Fan Jiahuan1,2, Cai Yu1,2, M.V. Reddy2,3* , K.P. Loh 3, B.V.R. Chowdari2

1 NUS High School of Mathematics and Science, 40 Clementi Avenue 1, Singapore 129959. 2Department of Physics, Advanced batteries lab/Graphene center, National University of Singapore, Singapore 117542.

3Department of Chemistry, Advanced batteries lab/Graphene center, National University of Singapore, Singapore 117542. corresponding Author : phymvvr@nus.edu.sg

This report includes studies of the effect of different preparation temperatures on the morphology, crystal structure and electrochemical properties of CuO. CuO materials were characterized by X-Ray Diffraction (XRD), Scanning Electron Microscopy (SEM) and Brunauer-Emmett-Teller (BET) surface area methods. Samples prepared under temperature of more than 510°C showed a single phase material with lattice parameter values of a=4.693Å, b=3.428Å, c=5.130Å and surface area with a range of 1.0-17.0 m2g-1. Electrochemical properties were evaluated via cyclic voltammetry (CV) and galvanostatic cycling studies. CV studies showed a minor difference in the peak potentials depending on preparation temperature and all compounds exhibited a main anodic peak at 2.45V and cathodic peaks at 0.85V and 1.25V. At a current rate of 60mAg-1 and in the voltage range between 0.005V and 3.0V, CuO prepared at 750°C showed a high and stable capacity of 620mAhg-1 at the end of 40th cycle.

## P2.8 Crystallographic structural refinements using computer software

Zhen Jie Low, Jia Hong Koh, Thanh Dung Pham Thi

Friday 12.30 PM, Foyer/Hallway, Panel 8

We explored the use of programs TOPAS & VESTA in crystallographic studies - refinements of X-ray diffraction (XRD) patterns and generation of unit cell images. Crystallographic models are employed to understand the structure of variety of crystalline of inorganic and organic materials. The crystal systems are broadly classified into 7 crystal systems, i.e. cubic, tetragonal, orthorhombic, rhombohedral, hexagonal, monoclinic and triclinic. We studied aspects of crystallography, both theory and experimental, 7 crystal systems, unit cell, theoretical evaluation of interplanar distances (d-values) etc. and solving the structures of inorganic compounds. The Rietveld refinement studies on selected simple and complex oxides were evaluated in detail. We calculated lattice parameters, positional occupancies and thermal parameters, Miller indices (hkl) planes, density etc. and visualized the atoms in a crystal lattice using both commercially and freely available computer programs. Also we demonstrated the simplicity of these computer programs in analyzing various different solids used in our daily life and the advantages of models in the area of physics, chemistry and materials and energy science.

## P2.9 Stuides on pure and Co-doped LiMn2O4 prepared by NaCl:KCl molten salt

Zhao Xuan, M V Reddy, B V R Chowdari, X H Liu

Friday 12.30 PM, Foyer/Hallway, Panel 9

A one pot molten salt method (MSM) has been used to synthesize pure and Co-doped (0.17) LiMn2O4 using 0.5NaCl: 0.5KCl eutectic melt for 6 h soaking time. The phases are characterized by X-ray diffraction (XRD), Rietveld refinement of the XRD data, Scanning Electron Microscope (SEM), density and Brunauer−Emmer−Teller (BET) surface area. Single-phase compounds with cubic spinel structure are obtained in all cases. The lattice parameter(a 8.23Å) of LiMn2O4 does not vary with the synthesis temperature from 750-850 °C,but the Co-doped compound shows a smaller value (a 8.21Å) as can be expected from ionic size consideration. SEM image shows 1-5 µm sized spherical particles with 20 nm nanosized aggregates. Electrochemical properties are evaluated at ambient and elevated (50 °C) temperatures in cells with Li-metal as the counter electrode by cyclic voltammetry (CV), and galvanostatic cycling. CV results showed a clear redox peaks around 3.9 /4.1 V and 4.0V / 4.2 V vs. Li and the former redox couple show higher peak-currents in the Co-doped LiMn2O4. Galvanostatic cycling at various C-rates in the voltage range, 3.5-4.3V vs. Li up to 100 cycles showed that Co-doping reduces, but not completely suppresses the capacity-fading.

## P2.10 Growth of Layer-Structured Germanium Diselenide Nanostructures towards Optoelectronic Device Application

Bablu Mukherjee, Eng Soon Tok, Chorng Haur Sow

Friday 12.30 PM, Foyer/Hallway, Panel 10

Germanium Diselenide (GeSe2) is one of the most important wide bandgap IV-VI semiconductors (Eg = 2.7 eV) with layered structure used in photoelectric devices, memory cells, and waveguides application. We report here the controlled synthesis of various high-quality GeSe2 nanostructures (nanowire, nanobelts, and stepped nanobelts) as well as other kinds of GeSe2 products (microbelts) via a simple vapor transport and deposition method. The photosensitivity of single GeSe2 nanobelt devices were examined with different excitation wavelengths of laser beams. A maximum photoconductive gain 46.4

## P2.11 Raman and resonance Raman study of ultrathin MoS2

Hong Li, Qing Zhang

Friday 12.30 PM, Foyer/Hallway, Panel 11

Raman and resonance Raman spectroscopy are employed to study ultrathin MoS2 flakes. It is found that the frequencies, widths and intensities of the Raman E12g (in-plane) and A1g (out-of-plane) peaks show strong dependence on the layer numbers of the ultrathin flakes. Nevertherless, only the frequencies of E12g and A1g peaks can be regard as the finger print of the layer number. The layer number identification using E12g or A1g peaks frequency are consistent with the characterization results from optical, atomic force microscopy and photoluminenscence. Resonance Raman spectra show that the coupling between electronic transition at point and phonon is weakened in ultrathin MoS2 in comparison with that in bulk MoS2, which is ascribed to the increased transition energy at K point due to the perpendicular quantum confinement or elongated intralayer atomic bonds. The asymmetric Raman feature centered at 454 cm-1 in bulk MoS2 is confirmed to be a combinational band involving LA(M) and A2u modes. Our results show that Raman spectroscopy is a reliable diagnostic tool to identify monolayer MoS2.

## P2.12 CHARGE TRANSPORT IN METAL-NANOCRYSTAL EMBEDDED GATE STACKS

Zin Zar Lwin, Kin Leong Pey, Qing Zhang

Friday 12.30 PM, Foyer/Hallway, Panel 12

The localized charge transport in metal-nanocrystal (MNC) embedded high-k/SiO2 gate stacks was investigated by Kelvin Force Microscopy characterization. The results clearly reveal that the lateral charge diffusion and vertical charge loss are two competing mechanisms and it strongly depends on the localized electric field of charged MNCs. From a comparative study of MNCs with different work function, it was found that the MNC with higher work function has smaller inter-dot tunneling probability which is favorable. However, the charge loss in initial decay period is a trade-off and it could be minimized by using dual-layer metal-NC structure. These observations can be incorporated into application of scaled memory devices with minimum defect related charge loss.

## P2.13 Charge Transfer Mechanisms of Metal Oxides and Modelling through Impedance Spectroscopy

Xu Hong Yun Yun, Marcus Ng Ng Kai Jie, Lim Yong Hui, M V Reddy

Friday 12.30 PM, Foyer/Hallway, Panel 13

The aim of this project is to model the charge transfer mechanisms of magnesium doped lithium cobalt oxide (LiCo0.97Mg0.03O2) and lithium cobalt oxide (LiCoO2) and to find out the variation of basic physical parameters like resistance and capacitance and Li-diffusion co-efficient of LiCo0.97Mg0.03O2 and lithium cobalt oxide (LiCoO2). It was hypothesized that LiCo0.97Mg0.03O2 is better based on impedance values. The coin cell was prepared using LiCo0.97Mg0.03O2, and then subjected to Electrochemical Impedance Spectroscopy (EIS) and Galvanostatic Intermittent Titration Technique

(GITT). Experimental nyquist plots are modeled with equivalent electrical circuits by the combination of different resistors, capacitors and Warburg elements modeled through the Z-view software. In our project, we used several models, such as the Nobili, Bhonke model but it was found out that our own model was the most accurate and thus the most suitable to understand the charge transfer mechanisms. The GITT results were used to calculate the diffusion rate of lithium ions. The results were then analyzed and compared. It was found that LiCo0.97Mg0.03O2 was a better choice to be used in lithium-ion coin cells, as it had higher lithium ion mobility as shown by the GITT results. Ion mobility refers to the ability for ions to move through a medium in response to an electric field.

## P2.14 Optical Property of Organic Microfiber

Van Duong Ta, Rui Chen, Handong Sun

Friday 12.30 PM, Foyer/Hallway, Panel 14

In this work, we demonstrate organic microfibers fabricated by directly tip-drawing from composite of polymethylmethacrylate (PMMA) and epoxy resin with tunable diameter ranges from 5 to 100 $\mu$m. The microfibers possess cylindrical shape and could emit different type of light via excitation when different gain materials such as dye or colloidal quantum dots were embedded into the microfibers. Especially, by incorporating approximately 2 mM Rhodamine 6G dye molecules into the microfibers, optically-pumped multi-mode and even single-mode lasing with quality factor as high as 8000 were observed at room temperature. The optical property is carefully analyzed, and the lasing mechanism is ascribed to whispering gallery modes (WGM). Field distribution of WGM inside the microfiber is numerically studied by finite element methods (FEM). The simulation illuminates a good image of the WGM cavity. Moreover, lasing performance and size-dependent lasing characteristics have been systematically examined, and the results show agreements with theoretical calculation.

## P2.15 Coupling of Topological Surface States in Ultrathin Sb (111) Films

Ziyu Luo, Feng Pan, Guanggeng Yao, Wentao Xu, Jiatao Sun, Hui Pan, Yuanping Feng, Xue-Sen Wang

Friday 12.30 PM, Foyer/Hallway, Panel 15

In the recent research on Topological Insulators, a group of materials such as Bi2Se3, Bi2Te3, and Sb2Te3 have been proved to be topological insulators by Angle-resolved photoemission spectroscopy (ARPES). According to the theoretical prediction in previous works, as one parent component of topological insulators, Sb single crystal has a nontrivial topological order. In our work, we studied the topological quantum states in ultrathin Sb (111) films by DFT calculations. Our calculation results show that, when the thickness of Sb ultrathin films is above 15 bilayers, two surface states with different spin are separated by bulk part, while the thickness is below 15 bilayers, a mixture of spin in the system occurs. This result can also fit our Fourier transform scanning tunneling spectroscopy experimental results very well.

The ultrathin Sb films, compared to bulk topological insulators, might have a good transport property because of less bulk proportion.

## P2.16 Structural properties of GaN grown on AlGaN/AlN stress mitigating layers on 100-mm Si (111) by ammonia molecular beam epitaxy

Manvi Agrawal, Dharmarasu Nethaji, K Radhakrishnan, Ravikiran Lingaparthi

Friday 12.30 PM, Foyer/Hallway, Panel 16

GaN based HEMTs are strong candidates for future high power and high frequency applications as they offer a unique combination of high saturation velocity and breakdown field. AlGaN/GaN HEMT structures have been widely demonstrated on Si substrate by metal organic vapor phase epitaxy and molecular beam epitaxy technique. This is due to the low cost, large size (up to 12 inch diameter) and easy availability of Si substrates. Furthermore, Si is an exclusive choice for microelectronics integration of GaN with its matured technology. However, the high lattice mismatch (17

GaN was grown on Al(0.45)Ga(0.55)N/AlN stress mitigating layers on thermally cleaned Si (111) substrate. A set of three samples: A, B and C were grown with 200nm AlN at 920 $^0$C followed by AlGaN at different growth temperatures of 840 $^0$C, 820 $^0$C and 800 $^0$C, respectively. For all the samples, the growth temperature of the top GaN was 800$^0$C, and the thickness of GaN and AlGaN was kept at 500 nm and 400 nm, respectively.

Poor quality and highly strained GaN was obtained at higher AlGaN growth temperatures. GaN grown on lower AlGaN growth temperatures showed an improved quality and reduced strain values, but, exhibited three dimensional growth mode. Si-diffusion from the substrate was observed via pipe diffusion mechanism which was assisted by threading dislocations. The dislocation bending and looping at the AlGaN/AlN interface was found to have significant influence on the dislocation density, strain and Si diffusion from the substrate in the GaN layer. In summary, a growth mechanism involving dislocation generation, evolution and interaction is found to have played a major role in determining the quality and strain states of the GaN grown on AlGaN/AlN stress mitigating layers grown on Si (111) substrates.

## P2.17 Plasmonic Nanoantenna Arrays for SERS and LSPR Biosensing

Stephanie Dodson, Shuzhou Li, Qihua Xiong

Friday 12.30 PM, Foyer/Hallway, Panel 17

The intense Raman signature of biomolecules located in the hotspots of plasmonic materials is an ideal fingerprint-like identification tool for ultra-sensitive biosensing using surface enhanced Raman scattering (SERS). Recently, we have successfully fabricated sub-5nm gaps between features of Au nanoantenna arrays using electron beam lithography (EBL). Modeling the antenna using the Discrete Dipole Approximation (DDA) we have simulated the surface plasmon resonance (SPR) and intensity of hotspots of multiple geometries of antenna. Imaging the antenna arrays using far-field transmission and Raman scattering spectroscopies we have explored the LSPR and electric field enhancement of multiple geometries of antenna. We predict that these antenna arrays will show unprecedented sensitivity in biosensing towards single molecule detection using both SERS and LSPR techniques.

## P2.18 The Complex Network of Taiwanese Earthquakes

Zheng Liu, Siew Ann Cheong

Friday 12.30 PM, Foyer/Hallway, Panel 18

Because Taiwan sits along the boundary between the Asia and Pacific tectonic plates, which are constantly colliding into each other, it experiences frequent earthquakes. These earthquakes vary in magnitudes, locations, and depths, but can be understood to relieve stresses that are accumulated through the motion of the tectonic plates. These earthquakes are also understood to occur along faults, such that one earthquake along a given fault triggers another earthquake along the same fault, or a second fault that is coupled to the first fault. Recently, some earth scientists have suggested viewing these faults as a complex network. In this poster, we apply the Abe-Suzuki and Baiesi-Paczuski complex network construction methods to map out the network of Taiwanese earthquakes. Through this study, we hope to understand more about the hierarchical organization of earthquakes, and their connections to faults.

## P2.19 Chemical Picture of Extreme Dynamics in the Singapore Stock Exchange

Boon Kin Teh, Siew Ann Cheong

Friday 12.30 PM, Foyer/Hallway, Panel 19

Market crashes are as abrupt and unpredictable as earthquakes. There is, however, an important distinct between the two. Whereas earth scientists are starting to get high-resolution data on a small number of important seismological variables, the financial markets have for a long time been blessed with large volumes of high-frequency data at the individual stock level. Drawing upon the much-lower-quality data of Tycho Brahe, Newton discovered the Three Laws of Motion. Why then have we not formulated the Three Laws of Market Dynamics? We believe the sheer volume of financial data available to us is as much a curse as a blessing, and that various forms of coarse graining is necessary before the human mind can grasp what goes on during market crashes. In this poster, we will report a time series clustering study of the Singapore Stock Exchange over various violent periods in recent history. We will explain how the price time series of different stocks can be clustered based on their Pearson correlations in a series of sliding windows. We then explain how the slow time evolution of the abundance and compositions of these clusters allow us to develop a chemical picture — involving the reaction and subsequent dissociation of various clusters — of market crashes in the Singapore Stock Exchange.

## P2.20 Cyclic Voltammetry and Space Charge Limited Current Mobility Measurement of Water-based Organic Solar Cells

Ma Ka Kui, Sum Tze Chien, Michael Kurniawan, Tai Kong Fai, Alfred Huan

Friday 12.30 PM, Foyer/Hallway, Panel 20

Water-based organic solar cells are important as to replace current popular organic solar cells based on poly (3-hexylthiophene) (P3HT) and the fullerene derivative [6,6 - phenyl - C61 - butyric acid methyl ester (PCBM) which involve toxic solvents such as chlorobenzene. Here we present some characterizations of 4 water soluble conjugated polymers poly[ 3- (potassium - 4 - butanoate) thiophene - 2,5-diyl], poly[3 - (potassium - 5 - pentanoate) thiophene - 2, 5- diyl], poly[3 - (potassium - 6 - hexanoate) thiophene - 2,5-diyl], poly[3- (potassium-7-heptanoate) thiophene-2,5-diyl] (abv. P4, P5, P6, P7) and a water soluble fullerene derivative C60(OH)24/26.

Cyclic Voltammetry Using cyclic voltammetry, the highest occupied molecular orbital (HOMO) for the polymers and lowest unoccupied molecular orbital (LUMO) for the fullerene derivative was found. It was found that the HOMO levels for the polymers were similar to that of P3HT, as -5.4 eV for P4 and P5, and about -5.1eV for P6 and P7, which is comparable to -5.2eV for P3HT. The bandgap for P6 and P7 are much smaller as the molecular weight is larger, which causes a larger delocalisation of electrons along the polymer chain, and thus valence and conduction bands broaden. The LUMO level for C60(OH)24/26 was found as -3.5eV, compared to -3.75eV for PCBM. The comparable values for the energy levels allows for selection of the correct blend to construct the optimum solar cell.

Space Charge Limited Current (SCLC) Using SCLC, the carrier mobility in the direction perpendicular to the plane of substrate was found. The hole mobility for the polymers was found to be of same order of magnitude to that of P3HT which is 10-4 cm2/Vs but the electron mobility of C60(OH)24/26 (8.90 x 10-7 cm2/Vs) was found to be 4 orders of magnitude lower than that of PCBM. We hereby conclude that one limiting factor to poor efficiency of blend solar cells was that the mobility of the acceptor was much lower than that of the donor, and hence causing inefficient separation of charges.

## P2.21 Transient absorption spectroscopy of CVD-grown graphene

Jingzhi Shang, Ting Yu, Gagik Gurzadyan

Friday 12.30 PM, Foyer/Hallway, Panel 21

Transient absorption spectra of monolayer, bilayer and stacked CVD-grown graphene films have been obtained in the visible range by UV pump/white-light probe spectroscopy. The wavelength dependences of carrier dynamics, including carrier-carrier, carrier-phonon and phonon-phonon scattering, were studied. The decay time, for all CVD-grown graphene samples, has a increasing tendency with increasing probed photon wavelength, i.e. the electrons at the lower excited level live longer compared with the ones at the higher energy level, analogous to those in graphite. In detail, the linear dependence of carrier decay rate on the probe photon energy was found and attributed to the dominant carrier-optical phonon intervally scattering and the linear density of states in the probed electronic band of graphene. Moveover, in the visible probe energy range, it is noted that the decay times in CVD-grown BLG are always slower than those in stacked two layer graphene and their differences become more obvious at lower probed photon energies. This phenomenon was explained by the slow carrier relaxation at the edges of the splitted electron bands of CVD-grown bilayer graphene, where the interband scattering channels were involved.

## P2.22 Highly ordered arrays of particle-in-bowl plasmonic nanostructure for Surface Enhanced Raman Scattering

Xianglin Li, Yongzhe Zhang, Shuzhou Li, Hongjin Fan

Friday 12.30 PM, Foyer/Hallway, Panel 22

Based on nanosphere lithography (NSL) and atomic layer deposition (ALD), a simple method is here proposed to fabricate a highly-ordered particle-in-bowl (PIB) nanostructure array that severs as a promising surface-enhanced Raman scattering (SERS) substrate. The PIB nanostructures are composed of size controlled Ag nanoparticles and gold nanobowls, which are separated with a controllable thickness of ALD dielectric thin layer. The SERS performance of the PIB arrays and the relationship with main parameters, including the Ag particle size and the ALD film thickness are characterized using 532 nm incident light. With Rhodmaine 6G as the probe molecule, the spatially averaged SERS enhancement factor is on the order of $4\times107$ and the local enhancement factor is much higher. The controlled size, tunable gap distance, and larger-area ordered arrays of these substrates suggest their promising applications as functional components in spectroscopy and biosensors.

## P2.23 Graphene Diode Based on Pseudospin Interaction in Closed-edge Bilayer Graphene

Jiaxu Yan, Da Zhan, Zexiang Shen

Friday 12.30 PM, Foyer/Hallway, Panel 23

Depending on the sublattices they propagate, the low-energy electrons or holes are labeled with pseudospins. By engineering the pseudospin interaction, we propose that two critical features of a diode, i.e. bandgap opening and spatial charge separation can be realized in graphene layers with proper stacking. We also demonstrate theoretically that such a graphene diode may play a role in the future pseudospin electronics, such as for harvesting the solar energy.

## P2.24 Surface Nanobubble Detection Using Total Internal Reflection Microscopy

Chan Chon U, Claus-Dieter Ohl

Friday 12.30 PM, Foyer/Hallway, Panel 24

Nanobubbles are surface attached gas cavities of pancake shape with tens of nanometer in height and of several 100 nm in diameter. Nanobubbles are found to be stable for many hours. From simple considerations of the Laplace pressure they should dissolve within milliseconds. This diffusion stability is an open research questions with some very recent models proposing a dynamic stability.

Typically, nanobubbles are probed with atomic force microscopy. This technique is a slow scanning method which can't resolve dynamics of these gas-liquid interfaces. Being able to detect the existence of surface nanobubbles on a faster time scale is necessary to study formation mechanisms and their stability. Here, we will present first results using total internal reflection microscopy (TIRF) technique to detect nanobubbles generated with the water-ethanol-water technique.

## P2.25 Guanine Base Stacking in G-quadruplexes: A Quantum Chemical study

Christopher Lech, Brahim Heddi, Anh Tuan Phan

Friday 12.30 PM, Foyer/Hallway, Panel 25

G-quadruplexes constitute a unique class of nucleic acid secondary structure characterized by stacked layers of planar guanine assemblies stabilized by a centralized cation, namely K+ or Na+. In G-quadruplexes, guanine bases from neighboring layers stack upon one another in a manner much different from that observed in duplex DNA and RNA. Individual G-quadruplex blocks also have a propensity to stack upon one another forming higher order aggregates. This interfacial stacking has consequences for naturally forming G-quadruplexes as well as engineered structures. This study uses a quantum chemical approach to understand how guanine base stacking influences higher order structure, specifically at the interface of stacked G-quadruplexes. A survey of guanine base stacking geometries found in experimentally reported structures is undertaken. Energy landscapes of stacked guanine assemblies are computed using both a quantum chemical and molecular dynamic force field approaches. The interaction energies of experimental base stacking geometries are evaluated using high level quantum chemical MP2 methods. Energy differences between base stacking modes are discussed with special attention paid to their implications towards high-order G-quadruplex assemblies.

### P2.26 ZnO-based dilute magnetic semiconductors for spintronics

Usman Ilyas, Rajdeep Rawat, Tuck Lee Tan, Paul Lee, Chen Rui, H.D Sun, Li Fengji, Sam Zhang

Friday 12.30 PM, Foyer/Hallway, Panel 26

The emerging field of spintronics represents the convergence of two fundamental properties of the electron charge and the electron spin to form the basis for a new class of device design. One of the ingenious ways to combine the spin and the charge of the carriers in a material is by synthesizing a material with both semiconducting as well as magnetic properties. This idea prompted the evolution of a new class of materials known as Dilute Magnetic Semiconductors (DMS), where a fraction of atoms in host semiconductor is substituted by ferromagnetic atoms of rare earth or transition metals to provide magnetic functionality. The II-VI based (ZnO) systems doped with Mn are well studied system for spintronic applications. The role played by the doping concentration and the structural defects towards the ferromagnetic ordering has been investigated. The ferromagnetic origin in narrow-size-distributed ZnO:Mn nanoparticles with oxygen rich stoichiometery was attributed to the strong p-d hybridization of Mn ions in ZnO host matrix, a pre-requisite for spintronic applications.

### P2.27 Bouncing Bubbles: thin films and their characterization

Herve Elettro, Maurice Hendrix, Claus-Dieter Ohl

Friday 12.30 PM, Foyer/Hallway, Panel 27

Sometimes seemingly simple problems reveal a rich physical world. One example is the rise and bounce of a small bubble (diameter ¡ 1mm) in a stagnant liquid from a solid wall. In experiments we record the shape of the bubbles and find that it is deforming during the bounce while a thin film of water remains between the bubble and the wall. The time to drain this film is much longer than the bounce. We explain the repulsion force with the surface tension "pulling" the bubble back to its undisturbed spherical shape and away from the wall. The thickness of the liquid film is only a few micrometers, yet its dynamics is crucial for the shape oscillation of the bubble. We study this thin film using two high-speed cameras, one two reveal the bubble shape and one to measure the thickness with interference. To capture the fringe pattern, recordings at more than 50,000 frames deemed necessary. The interference pattern reveals the formation of a dimple at the center of the impact region as predicted by a lubrication model. The more complex problem of an oscillating bubble rising towards a wall, which is of interest in bubble cleaning applications, along with a theoretical model describing the dynamic of the thin film are in progress.

## P2.28 Anisotropic charge carrier photogeneration and transport in rubrene single crystals

Zilong Wang, Xin Yu Chin, Ke Ke Zhang, Christian Kloc, Cesare Soci

Friday 12.30 PM, Foyer/Hallway, Panel 28

Molecular single crystals are extensively considered as a model system for the charge carrier photogeneration and transport properties of organic semiconductors. In particular two proposed mechanisms for charge carrier photogeneration, namely direct polaron generation and exciton dissociation, have been widely debated in the literature. The anisotropic optical and charge transport properties of highly ordered rubrene crystals allow independent tuning of the optical penetration depth and the selection of polarized dipole transitions relative to the molecular axis, and provide a mean to decouple the contributions of surface and bulk states. We have conducted polarized photoinduced absorption measurements in the near-infrared spectral region to probe the polaron density, as well as photoconductivity and air-gap phototransistor measurements to study the anisotropic transport properties of rubrene single crystals. We find that oxidized surface states and bulk states have unique spectral polarization signatures, which will be discussed in the context of exciton diffusion and polaron dynamics.

## P2.29 Accelerating droplets with an electromagnetic gun

Simon Xinyi Chua, Claus-Dieter Ohl

Friday 12.30 PM, Foyer/Hallway, Panel 29

Impacting droplets at high velocities are used in many spray related applications, for example in spray cleaning and for spray painting. A good understanding on the fluid mechanics during the droplet impact is needed to reduce the side effects which may be the damaging of surface structures while enhancing the efficiency of the process. One obstacle in this research effort is the generation of single high-speed droplets of sufficient large size to be easily studies. The acceleration of small droplets to 10-20 m/s can easily be accomplished with current ink-jet printer technology; however large droplets tend to fragment. Rain droplets for instance, may only reach a few meters per seconds as their terminal velocity. Here, we present a novel experiment which allows for much faster droplets: We use an iron projectile housing the droplet. The projectile is accelerated using a coil gun by discharging a bank of capacitors rapidly through a low Ohmic resistance coil. Then, the projectile bearing a droplet of liquid is abruptly stopped while the droplet continuous to move with its momentum gained. We present results of our study on the motion of the projectile and the droplet using high-speed camera recording.

## P2.30 Charge Modulation Spectroscopy of Conjugated Polymers in the Medium Infrared

Xin Yu Chin, Zilong Wang, Jun Yin, Heinrich Diesinger, Mario Carioni, Cesare Soci

Friday 12.30 PM, Foyer/Hallway, Panel 30

Charge Modulation Spectroscopy (CMS) is an electro-optical method that allows probing the gate-induced charge carrier density in the channel of a working Organic Field Effect Transistors (OFETs). Here we study CMS of a common conjugated polymer, regio-regular poly(3-hexylthiophene) (rr-P3HT), by probing the Infra-Red Active Vibrational (IRAV) modes due to the polarons induced by electrostatic doping. Electro-induced reflectance spectra are acquired between 800 and 4000 wavenumbers and compared to photoinduced IRAV spectra, showing a one-to-one correspondence between vibrational modes. Mapping of the charge-transfer bands by confocal IR microscopy shows the spatial distribution of polarons injected in the channel when a source-drain voltage is applied. This demonstrates the potential of CMS in the medium infrared spectral region to characterize charge carrier generation, injection, transport, and possibly dynamics in working OFETs.

## P2.31 Enhanced Optical Dichroism of Graphene Nanoribbon

Fábio Hipólito

Friday 12.30 PM, Foyer/Hallway, Panel 31

The optical conductivity of graphene nanoribbons is analytical and exactly derived. It is shown that the absence of translational invariance along the transverse direction allows considerable intra-band absorption in a narrow frequency window that varies with the ribbon width, and lies in the THz range domain for ribbons 10-100nm wide. In this spectral region the anisotropy in the optical conductivity can be as high as two orders of magnitude, which renders the medium dichroic, and allows near 100% degree of polarization with just a single layer of graphene.

## P2.32 Ultra hard TiC coating using dense plasma focus

Zeshan Adeel Umar, Rajdeep Rawat, Riaz Ahmad, K. S. Tan, Arjun Krishna Kumar, Zhong Chen, Lu Shen

Friday 12.30 PM, Foyer/Hallway, Panel 32

Hard nanocomposite titanium carbide films were synthesized on silicon substrate using dense plasma focus device (DPF). The TiC thin films have been deposited using different concentration of argon and methane. The deposited films were then characterized using XRD and SEM to see the composition, structure and surface morphology respectively. XRD patterns confirmed the formation of TiC composites on silicon substrates. SEM Analysis showed that the film consist of nano size particles. Raman Analysis is done to check the presence of a-C in the films treated with different Ar/CH4 ratio. The presence of D and G peaks for the film treated with higher concentration of methane showed the presence of a-C. Hardness of the deposited films with different Ar/CH4 ratio was also measured.

## P2.33 Localization behavior of Dirac particles in disordered graphene superlattices

Qifang Zhao, Jiangbin Gong, Cord Mueller

Friday 12.30 PM, Foyer/Hallway, Panel 33

Graphene superlattices (GSLs), formed by subjecting a monolayer graphene sheet to a periodic potential, can be used to engineer band structures and, from there, charge transport properties, but these are sensitive to the presence of disorder. The localization behavior of massless 2D Dirac particles induced by weak disorder is studied for both scalar-potential and vector-potential GSLs, computationally as well as analytically by a weak-disorder expansion. In particular, it is investigated how the Lyapunov exponent (inverse localization length) depends on the incidence angle to a 1D GSL. Delocalization resonances are found for both scalar and vector GSLs. The sharp angular dependence of the Lyapunov exponent may be exploited to realize disorder-induced ltering, as veried by full 2D numerical wave packet simulations.

## P2.34 Electric Field-Dependent Photoconductivity in CdS Nanowires and Nanobelts: Exciton Ionization, Franz-Keldysh and Stark Effects

Dehui Li, Jun Zhang, Qing Zhang, Qihua Xiong

Friday 12.30 PM, Foyer/Hallway, Panel 34

We report on the electric field dependent photoconductivity (PC) near the band edge region of individual CdS nanowires and nanobelts. The quasi-periodic oscillations above the band edge in nanowires and nanobelts have been attributed to a Franz-Keldesh effect. The exciton peaks in photoconductivity spectra of the nanowires and thinner nanobelts show pronounced red shifting due to the Stark effect as the electric field increases, while the excitons ionization is mainly facilitated by strong electron-longitudinal optical (LO) phonon coupling. However, the band edge transition of the thicker nanobelts blue shifts due to the field enhanced exciton ionization, suggesting partial exciton ionization as the electron-LO phonon coupling is suppressed in the thicker belts. Large Stark shifts, up to 48 meV in the nanowire and 12 meV in the thinner nanobelts, have been achieved with moderate electric field strength on the order of kV/cm, indicating a strong size and dimensionality implication due to confinement and surface depletion.

# 6 Talks

## 6.1 T2 Semiconductor Light Sources/Econophysics

This session on "Semiconductor Light Sources/Econophysics" will be held on Thursday, February 23, from 11.00 AM to 12.30 PM. The venue for this session is Lecture Theatre LT31. Time allocated for invited talks is 25 min speaking time, plus 5 min questions, and time allocated for contributed talks is 12 min speaking time plus 3 minutes questions.

### T2.1 Recent progresses @ Luminous! Center of Excellence for Semiconductor Lighting and Displays (INVITED)

Xiao Wei Sun

Thursday, February 23, 11.00 AM, Lecture Theatre LT31

In this presentation, I would like to introduce some recent progresses at Luminous! Center of Excellence for Semiconductor Lighting and Displays. Especially, we established a III-nitride based light-emitting diode (LED) program and obtained high quality epi-layers and good performance LEDs. Progresses were also made in organic tandem organic light-emitting diodes, organic photovoltaic devices, ZnO LED and lasing, and electrochromics based smart windows.

### T2.2 High Performance Quantum Cascade Lasers: semiconductor lasers for mid-infrared and Terahertz (INVITED)

Qijie Wang

Thursday, February 23, 11.30 AM, Lecture Theatre LT31

Quantum cascade laser (QCL) is a new class of semiconductor laser based on multiple quantum wells/barriers designed to emit light in the mid-infrared and Terahertz ranges, roughly from 3 – 300 um. Because the emission wavelength of this device is not determined by the bandgap of the material but by suitable engineering the thicknesses of those multiple quantum wells/barriers, it has been widely used to generate arbitrary wavelength emission in the mid-infrared and Terahertz for various applications, including but not limited to, chemical sensing, spectroscopy, imaging, security and defense, astronomy science, and free-space communications.

In this talk, I will first introduce the operation principle of QCLs. Then I will talk about what is the design difference between the mid-infrared and THz QCLs and the challenges. After that, I will introduce what we have done so far to improve the output power level, threshold current, and dynamic range of mid-infrared QCLs, and to achieve high temperature operation of THz QCLs. Performance with peak output power more than 1 W and slope efficiency of 1 W/A has been achieved for devices with an emission wavelength of 9 um at room temperature. Devices emitting at a wavelength around 5 um shows continuous-wave output power more than 1 W at room temperature with a single laser chip. In the end, a few applications of QCLs will be reviewed.

### T2.3 Understanding the Dynamics of Complex Systems from High-Frequency Time Series Data (INVITED)

Siew Ann Cheong

Thursday, February 23, 12.00 PM, Lecture Theatre LT31

Complex systems are characterized by a multitude of strongly interacting time and length scales that differ by many orders of magnitude. One of the grand visions of complexity study is to start with a microscopic description at the smallest time and length scales, and understand how effective descriptions at larger time and length scales emerge one after another. In this talk, I will describe two complementary approaches based on high-frequency time series data generated by real-world measurements or through computer simulations. In the (1) time series segmentation method, we break a statistically non-stationary time series into statistically stationary segments. By clustering the large number of time series segments, we obtain a higher-level description of the dynamics in terms of a small number of macroscopic phases. By analyzing the cross section of microscopic variables, we can then further determine how quickly each macroscopic phase propagates through the system, and the lifetimes of these phases. To illustrate this method, I will talk about our attempts to understand stock market dynamics in the US economy, and also the folding dynamics of a small protein. Where the time series segmentation method is particularly well suited to the quantitative determination of effective dynamical time scales, the (2) time series clustering method allows us to discover the effective variables associated with these macroscopic time scales. To do so, we compute cross correlations between microscopic variables over a long-time window, and then group the most strongly correlated microscopic variables into effective variables. Furthermore, by sliding the long-time window across the data set, we can understand how effective variables evolve on a slower time scale. As examples, I will show the slow time evolutions of effective variables that the method discovered, for the Singapore Stock Exchange across the Sep 2008 Lehman Brothers crisis, and for the Sumatra GPS network across the Dec 2007 M-8.5 earthquake.

### 6.2 T3 Thin Films

This session on "Thin Films" will be held on Thursday, February 23, from 11.00 AM to 12.30 PM. The venue for this session is Seminar Room 03-07. Time allocated for invited talks is 25 min speaking time, plus 5 min questions, and time allocated for contributed talks is 12 min speaking time plus 3 minutes questions.

#### T3.1 Atomic Layer Deposition for Nanofabrication and Interface Engineering (INVITED)

Hongjin Fan

Thursday, February 23, 11.00 AM, Seminar Room 03-07

Atomic layer deposition (ALD) is a vapor-phase thin film growth technique that allows atomic-scale thickness and uniformity control, particularly on high aspect-ratio nanostructures. It has become a technique for both template-directed nanofabrications and engineering of surface properties. This talk will highlight the recent application of ALD in selected fields including photonics, SERS and energy materials. Specifically, the topics include fabrication of plasmonic nanostructures for the SERS applications, fabrication of 3-D nanoarchitectured photoanodes for solar energy conversions (dye-sensitized solar cells and photoelectrochemical cells), and coating of electrodes to enhance the cyclic stability and thus device life span of batteries. Dielectric coating for tailoring optical properties of semiconductor nanostructures is also discussed as exemplified by ZnO nanowires.

#### T3.2 Fabrication and Characterization of Ultrathin Oxide Films and Super-lattices Epitaxially Using Laser Molecular Beam Epitaxy (INVITED)

Weiguang Zhu

Thursday, February 23, 11.30 AM, Seminar Room 03-07

In very recent years, multifunctional ultrathin epitaxial oxide films and superlattices have attracted great interests, intensive research works have been carried out to answer fundamental and scientific challenges, and to seek huge opportunities and potential in electronic device applications. Specific attention has been paid to those multifunctional ultrathin oxide films and superlattices epitaxially grown by laser molecular beam epitaxy technique (L-MBE), which is able to deposit films and superlattices of oxides and ceramics with very high melting temperatures at surface smoothness down to atomic level. In this paper, fully strained multiferroics superlattices: [(La0.8Sr0.2MnO3) 4n/ (BaTiO3) 3n]m superlattices, where n = 1, 2, 3 and 4, and m is integer number from 1 to 16, were grown on SrTiO3 (001) single crystal substrates using L-MBE. The two-dimensional layer-by-layer growth was in situ monitored by reflection high energy electron diffraction (RHEED); structural, electrical and magnetic properties these thin films were systematically investigated. Scanning probe and piezo-force microscopy were also employed to characterize ultrathin ferroelectric films on LSMO substrate to study the polarization and switching effects on the interfacial charge states, ferroelectric tunneling junction, and giant electro-resistance phenomena. Metal oxide SnO2 thin films were also epitaxially grown on various oriented sapphire and SrTiO3 (100) single crystal substrates. In 5% Fe doped SnO2, magnetization was increased by Mg p-type doping, but decreased with Sb n-type electron doping, in consistent with the spin change; and the related electrical conduction behaviors and mechanisms due to p- and n-doping in these SnO2 epitaxial films were also studied. The interesting thickness effect on electric conduction in SnO2 thin films was observed: metallic conduction in thicker films was transferred to insulating conduction when the film thickness downed to about 3.1 nm. The experiment results will be presented and the fundamental mechanisms will be discussed.

### T3.3 Spin-momentum helical locking induced spin-valve effects in topological insulator/ferromagnet heterostructures

Bin Xia, Zhipeng Li, Peng Liu, Peng Ren, Haibin Su, Alfred Huan, Zhili Dong, Lan Wang

Thursday, February 23, 12.00 PM, Seminar Room 03-07

Topological insulator is composed of an insulating bulk state and an odd number of massless spin-helical Dirac cone formed two-dimensional surface state. Here, we report a novel spin-valve effect in Bi1.5Sb0.5Te1.8Se1.2/CoFe heterostructures. This effect indicates the spin-momentum helical locking on the Bi1.5Sb0.5Te1.8Se1.2 topological surface state. It is also indicated that the characteristics of helical surface can be preserved at topological insulator/ferromagnet interface although the ferromagnetism can break the time reversal symmetry and therefore generate an energy gap at the topological Dirac point.

### T3.4 Growth of single-crystalline CdSe thin films studied by scanning tunneling microscopy

Guanggeng Yao, Feng Pan, Wentao Xu, Ziyu Luo, Xue-Sen Wang

Thursday, February 23, 12.15 PM, Seminar Room 03-07

Wurtzite-structured cadmium selenide (CdSe) is an important II-VI semiconducting compound for optoelectronics, and CdSe quantum dots have drawn much attention as typical nanostructures to study the quantum confinement effect. However, up to now, only a few studies can be found in literature studying the growth of single-crystalline CdSe films. Here the kinetic growth process of CdSe on Si(111)-$\sqrt{3}\times\sqrt{3}$:Bi-β surface is investigated using Auger electron spectroscopy, low-energy electron diffraction and scanning tunneling microscopy. Atomically smooth, single crystalline CdSe thin films can be obtained by physical vapor deposition in ultra high vacuum conditions, following the Frank-Van der Merwe mode along (0001) direction. Besides, detailed measurements on the reconstruction of (0001) surfaces are performed, revealing the 2×2 reconstruction by STM for the first time, which is in good agreement with our theoretical calculations.

## 6.3 T4 THz Physics

This session on "THz Physics" will be held on Thursday, February 23, from 11.00 AM to 12.30 PM. The venue for this session is Seminar Room 03-04. Time allocated for invited talks is 25 min speaking time, plus 5 min questions, and time allocated for contributed talks is 12 min speaking time plus 3 minutes questions.

### T4.1 THz Spectroscopy of Semiconductor Nanostructures (INVITED)

Xinhai Zhang

Thursday, February 23, 11.00 AM, Seminar Room 03-04

Terahertz (THz) wave refers to electromagnetic radiation in the frequency interval from 0.1 to 10 THz. THz spectroscopy has the advantage of probing nanostructures and bulk materials that are difficult to contact. THz time-domain spectroscopy (THz-TDS) is a powerful tool to study materials properties such as complex dielectric response and conductivity in the far-infrared spectral region, with the advantages of high signal-to-noise ratio, noncontact optical probe, and measuring the amplitude and phase of electric field simultaneously thus no requirement for Kramers-Kronig transformation. The optical pump-THz probe (OPTP) spectroscopy has recently emerged as a powerful technique to study the ultrafast carrier dynamics of materials. In OPTP, the photon energy of THz probe is in the range of meV (1 THz = 4.1 meV), naturally matching the energy scale of elementary excitation in solids (i.e., excitons). OPTP can measure the carrier population and transient conductivity, supplying information for carrier generation, exciton formation/dissociation, carrier thermalization and cooling, as well as carrier recombination. These informations are very important for both fundamental physics and device applications. Using THz-TDS and OPTP, we study the complex dielectric property, complex conductivity, and ultrafast carrier dynamics of CdS, CdSeS, and Si nanostructures. These materials are technologically important for device applications. Interesting carrier dynamics in these materials will be presented and discussed.

### T4.2 Theoretical investigation of injection-locked high modulation bandwidth quantum cascade lasers

Bo Meng, Qijie Wang

Thursday, February 23, 11.30 AM, Seminar Room 03-04

In this study, we report for the first time to our knowledge theoretical investigation of modulation responses of injection-locked mid-infrared quantum cascade lasers (QCLs) at wavelengths of 4.6 μm and 9 μm, respectively. It is shown through a three-level rate equations model that the direct intensity modulation of QCLs gives the maximum modulation bandwidths of 7 GHz at 4.6 μm and 20 GHz at 9 μm . By applying the injection locking scheme, we find that the modulation bandwidths of up to 30 GHz and 70 GHz can be achieved for QCLs at 4.6 μm and 9 μm , respectively, with an injection ratio of 5 dB. The result also shows that an ultrawide modulation bandwidth of more than 200 GHz is possible with a 10 dB injection ratio for QCLs at 9 μm. An important characteristic of injection-locked QCLs is the nonexistence of unstable locking region in the locking map, in contrast to their diode laser counterparts. We attribute this to the ultra-short upper laser state lifetimes of QCLs.

### T4.3 Llinewidth broadening caused by intrinsic temperature fluctuations in mid-infrared quantum cascade lasers

Tao Liu, Qijie Wang

Thursday, February 23, 11.45 AM, Seminar Room 03-04

We theoretically investigate fundamental thermal frequency noise and linewidth broadening caused by intrinsic temperature fluctuations in mid-infrared quantum cascade lasers (QCLs) for the first time. The analytical derivation is based on the Green function analysis and the Van Vliet-Fassett theory. The results show that the fundamental frequency noise caused by temperature fluctuations is prominent in the low frequency range (below a few kHz) and is sensitive to the temperature, heat conductivity and the thickness of the active region/substrate. It also shows that this fundamental frequency noise does not show a 1/f trend in the whole frequency spectra. This frequency noise leads to the linewidth broadening from 14.74 Hz to 62.02 Hz as the temperature increases from 200 K to 400 K. When the microscopic features of the refractive index variations associated with the intersubband gain transition, the self-heating-induced thermal expansion and energy level broadening in mid-IR QCLs are considered, an estimation shows that the linewidth broadening increases greatly by a factor of at least 4 times.

### T4.4 Terahertz properties of Tm (Tm=Cu, Ag) doped ZnO thin films

Mi He, Xingquan Zou, Yufeng Tian, Saritha Nair, Tom Wu, Elbert Chia

Thursday, February 23, 12.00 PM, Seminar Room 03-04

ZnO has attracted great attention because of potential applications in electro-optic, acousto-optic, and optoelectronic devices. With proper doping, the conductivity and transparency of ZnO can be tuned to a certain spectral region. Here, the optical and dielectric properties of Zn0.95Tm0.05O (Tm=Cu, Ag) thin films are studied by terahertz time-domain spectroscopy (THz-TDS) at different temperatures (10K - 300K) in the frequency range extending from 0.22 - 3 THz. The measured complex dielectric response and conductivity are well theoretically fitted. Comparing with undoped ZnO thin films, the doping effect of Ag and Cu is investigated.

### T4.5 Temperature-Dependence in Optical Properties of Topological Insulator $Bi_{1.5}Sb_{0.5}Te_{1.8}Se_{1.2}$

Chi Sin Tang, Xing Quan Zhou, Bin Xia, Mingyi Liao, Lan Wang, Elbert Ee Min Chia

Thursday, February 23, 12.15 PM, Seminar Room 03-04

Topological Insulators are materials with insulating bulk states and conducting states on their edge or surface. Using Terahertz Time-Domain Spectroscopy (THz-TDS), we studied the temperature-dependence of the optical properties of $Bi_{1.5}Sb_{0.5}Te_{1.8}Se_{1.2}$

single-crystals from 5 K to 300 K in the terahertz regime (0.4 THz to 3.0 THz). We observed a spectral weight shift from low frequencies to frequencies above 1.0 THz in the real conductivity at temperatures below $\sim$100 K.

## 6.4 T5 Nanofabrication/Graphene Electronics

This session on "Nanofabrication/Graphene Electronics" will be held on Thursday, February 23, from 02.00 PM to 03.30 PM. The venue for this session is Lecture Theatre LT31. Time allocated for invited talks is 25 min speaking time, plus 5 min questions, and time allocated for contributed talks is 12 min speaking time plus 3 minutes questions.

### T5.1 Chemically Enabled Nanofabrication for Nanoelectronics (INVITED)

Xiaodong Chen

Thursday, February 23, 02.00 PM, Lecture Theatre LT31

Nanofabrication is the foundation and enabler of the entire field of nanotechnology and nanoscience. For any nanofabrication method to be useful, simplicity and scalability must be considered. Here, I would like to give an overview of our recent efforts on chemically enabled nanofabrication, especially for their related work with nanoelectronics. I will address how the topography and molecule template directed methods were applied to form one-dimensional nanowires with unique electrical performance. In addition, I will show how we used a chemistry-based nanofabrication technique, on-wire lithography, to build molecular transport junctions, which are essential structures for developing the field of molecular electronics.

### T5.2 Synthesis of Epitaxial Non-planar Nanostructures on (001) Muscovite Mica via van der Waals Epitaxy

Muhammad Iqbal Bakti Utama, Qing Zhang, Francisco J. Belarre, Cesar Magen, Shuangfeng Jia, Dehui Li, Bo Peng, Jianbo Wang, Jordi Arbiol, Qihua Xiong

Thursday, February 23, 02.30 PM, Lecture Theatre LT31

Epitaxial nanostructure served as a unique platform to study various physical phenomena emerging at the nanoscale and to develop a novel device concept with enhanced performance and functionalities. However, despite the improved ability of nanostructures to relax strain elastically, a well-crystalized epitaxy of nanostructure is still strongly dependent on the lattice matching of the material with the substrate. Thus, the variation of materials for epitaxial growth is restrained by the availability of appropriate substrates in homoepitaxy and limited combinations of heteroepitaxy. An epitaxy approach called van der Waals epitaxy circumvent such limitation by utilizing layered substrates such that the heterointerface is connected via a weak van der Waals interaction instead of covalent chemical bonds, as typical in a conventional heteroepitaxy. We show that, by utilizing only (001) muscovite mica substrates in a catalyst-free vapor transport technique, the van der Waals epitaxy enabled the growth of non-planar epitaxial nanoarchitectures such as (i) vertically aligned nanowire arrays, (ii) nanotripods, (ii) and nanotetrapods with excellent crystallinity. Various binary semiconductors (e.g., ZnO, ZnS, ZnTe, CdS, CdSe, PbS, and GaN) can be prepared via the van der Waals epitaxy regardless of the ensuing lattice mismatch between those compounds and the muscovite mica substrate. Cross-sectional electron microscopy observations further revealed that the epitaxy is of incommensurate nature, which we believe to be responsible in alleviating the lattice matching requirement. These results effectively illustrate the versatility of the van der Waals epitaxy strategy, and the possibility for the preparation of other nanoarchitectures with higher complexity, such as hierarchical and heterostructures, on various other combinations of materials and layered substrates toward a broad range of promising technological applications.

### T5.3 Graphene Optoelectronics (INVITED)

Wei Ji

Thursday, February 23, 02.45 PM, Lecture Theatre LT31

Since graphene was made available by the Manchester group in 2004, it has become a new playground for scientists and engineers who would like to demonstrate their new ideas for next-generation optoelectronic devices. One of these ideas is the coherent control and noncontact generation of ballistic photocurrent in graphene via quantum interference between one-photon absorption and two-photon absorption. The other idea is the graphene-based photodetector with highly efficient, broadband, and ultrafast response to light signal. In this talk, we will present our progress at these two frontiers of scientific research.

### T5.4 Electrochemical Reduction and Re-oxidation of Graphene Oxide

Ye Tao, Hao Fatt Teoh, Chorng Haur Sow

Thursday, February 23, 03.15 PM, Lecture Theatre LT31

Reduced graphene oxide (rGO) is widely suggested as a new electronic material for its high conductivity and ease of synthesis. Its electrochemical behavior is therefore an interest for study. Here we investigated the reversible reduction of graphene oxide via direct electrical current to probe the mechanism of the conversion between GO and rGO. For reduction through electric current, it was found that 3 10 V potential difference applied between 10µm space lead to change in sample color starting from the negative terminal. The color change is indicative of GO reduction and confirmed via XPS. The reduction could be reversed by applying a reverse voltage. Reduction in film thickness was also observed in the reduced area. Metal deposits seemed to enhance the effect of reduction probably due to its rich supply of free electrons. The reduction is mainly attributed to electrochemical process due to supplied electron and access proton in trapped moisture. Electrical potential difference can also reverse laser-induced reduction of GO. The electrically reduced sample showed fractal patterns similar to dielectric breakdown. Laser-reduced GO between electrodes behave differently depending on position, closer to negative electrodes, reduction occurs; but closer to positive electrodes it is oxidized.

## 6.5 T6 Quantum Physics

This session on "Quantum Physics" will be held on Thursday, February 23, from 02.00 PM to 03.30 PM. The venue for this session is Seminar Room 03-07. Time allocated for invited talks is 25 min speaking time, plus 5 min questions, and time allocated for contributed talks is 12 min speaking time plus 3 minutes questions.

### T6.1 Wandering in "quantum control" and "nonlinear dynamics" (INVITED)

Jiangbin Gong

Thursday, February 23, 02.00 PM, Seminar Room 03-07

I will introduce recent research activities in my theoretical research group working on quantum control and nonlinear dynamics. Quantum control is not only necessary to realize future quantum technologies but also a fruitful area where we can freely explore new aspects of quantum dynamics and nonlinear physics. Due to time consideration I only describe two specific directions in detail. The first direction is to use cold-atom systems to explore implications of fractal Floquet spectrum as well as topological quantum phase transitions in driven quantum systems. Along this direction we discovered the possibility of long-lasting quantum exponential behavior and quantized adiabatic pumping in momentum space. The second direction is on aspects of open quantum systems. In particular, recently my students and I proposed to use dynamical decoupling fields to universally protect quantum entanglement.

### T6.2 Ferronematic order in a spin-1 Heisenberg antiferromagnet

Keola Wierschem, Pinaki Sengupta

Thursday, February 23, 02.30 PM, Seminar Room 03-07

We study the ground state phase diagram of a spin-1 Heisenberg antiferromagnet. The effects of an external magnetic field and easy-axis single-ion anisotropy are considered. In the case of large easy-axis single-ion anisotropy, direct spin-wave treatment predicts a single first-order phase transition from an antiferromagnetic ground state to a fully polarized ground state under increasing external magnetic field. Mean field arguments based on a spin-1/2 effective model, however, show that this transition is superseded by an intermediate phase with ferronematic order. This effective model becomes exact as the magnitude of the easy-axis single-ion anisotropy approaches infinity. Using exact diagonalization and quantum Monte Carlo methods, we demonstrate the existence of the intermediate phase and confirm the presence of ferronematic order.

### T6.3 Sharpening Occam's Razor with Quantum Mechanics

Mile Gu, Karoline Wiesner, Elisabeth Rieper, Vlatko Vedral

Thursday, February 23, 02.45 PM, Seminar Room 03-07

Mathematical models are an essential component of quantitative science. They generate predictions about the future, based on information available in the present. In the spirit of Occam's razor, simpler is better; should two models make identical predictions, the one that requires less input is preferred. Yet, for almost all stochastic processes, even the provably optimal classical models waste information. The amount of input information they demand exceeds the amount of predictive information they output. We systematically construct quantum models that break this classical bound, and show that the system of minimal entropy that simulates such processes must necessarily feature quantum dynamics. This indicates that many observed phenomena could be significantly simpler than classically possible should quantum effects be involved.

### T6.4 No-signaling Principle Can Determine Optimal Quantum State Discrimination

Joonwoo Bae, Won-Young Hwang, Yeong-Deok Han

Thursday, February 23, 03.00 PM, Seminar Room 03-07

We provide a general framework of utilizing the no-signaling principle in derivation of the guessing probability in the minimum-error quantum state discrimination. We show that, remarkably, the guessing probability can be determined by the no-signaling principle. This is shown by proving that in the semidefinite programming for the discrimination, the optimality condition correponds to the constraint that quantum theory cannot be used for superluminal communication. Finally, a general bound to the guessing probability is presented in a closed form.

### T6.5 Explicit capacity-achieving receivers for optical communication and quantum reading

Saikat Guha, Si Hui Tan, Mark M. Wilde

Thursday, February 23, 03.15 PM, Seminar Room 03-07

Abstract—An important practical open question has been to design explicit, structured optical receivers that achieve the Holevo limit in the contexts of optical communication and "quantum reading." The Holevo limit is an achievable rate that is higher than the Shannon limit of any known optical receiver. We demonstrate how a sequential decoding approach can achieve the Holevo limit for both of these settings. A crucial part of our scheme for both settings is a non-destructive "vacuum-or-not" measurement that projects an n-symbol modulated codeword onto the n-fold vacuum state or its orthogonal complement, such that the post-measurement state is either the n-fold vacuum or has the vacuum removed from the support of the n symbols' joint quantum state. The sequential decoder for optical communication requires the additional ability to perform multimode optical phase-space displacements—realizable using a beamsplitter and a laser, while the sequential decoder for quantum reading also requires the ability to perform phase-shifting (realizable using a phase plate) and online squeezing (a phase-sensitive amplifier).

## 6.6 T7 Graphene I

This session on "Graphene I" will be held on Thursday, February 23, from 04.00 PM to 05.30 PM. The venue for this session is Lecture Theatre LT31. Time allocated for invited talks is 25 min speaking time, plus 5 min questions, and time allocated for contributed talks is 12 min speaking time plus 3 minutes questions.

### T7.1 The soul of graphene ribbon (INVITED)

Chang Q Sun

Thursday, February 23, 04.00 PM, Lecture Theatre LT31

From the perspectives of interatomic bonding and electronic configuration, this presentation aims to show that the atomic-undercoordination-facilitated bond contraction, quantum entrapment of charge and energy, and the polarization of the unpaired sp2 electrons of the dangling bond dictate the anomalies demonstrated by graphene. Theoretical reproduction of the experimentally observed melting point depression, elastic modulus enhancement,1 strain and layer-number dependence Raman shift,2, 3 C 1s core-level shift,4 band gap expansion,5 edge and defect Dirac fermions generation6 and the associated magnetism confirmed consistently that the shorter and stronger bonds between undercoordinated carbon atoms modulate locally the atomic cohesive energy and the Hamiltonian which determine the variation of the detectable properties of bulk carbon.7 However, the polarization of the sp2 dangling-bond electrons by the densely entrapped core and bonding electrons generates the observed Dirac fermions at sites surrounding defects and edges. The weakly bounded edge fermions follow neither the standard dispersion nor occupy the allowed energy states in the valence band and below but they generate the midgap magnetic states that are almost massless and extremely mobile.8 It has been confirmed that the C-C bond contracts by up to 30% facilitated with 150% potential well depression at the edges with respect to those in the bulk diamond.

1 Sun, C.Q., et al., Dimension, strength, and chemical and thermal stability of a single C-C bond in carbon nanotubes. J. Phys. Chem. B, 2003. 107: 7544-6.

2 Zheng, W.T. and C.Q. Sun, Underneath the fascinations of carbon nanotubes and graphene nanoribbons. Energy & Environ Sci, 2011. 4: 627-55.

3 Yang, X.X., et al., Raman spectroscopic determination of the length, strength, compressibility, Debye temperature, elasticity, and force constant of the C-C bond in graphene. Nanoscale, 2011. DOI:10.1039/C1NR11280E.

4 Sun, C.Q., et al., Coordination-Resolved C-C Bond Length and the C 1s Binding Energy of Carbon Allotropes and the Effective Atomic Coordination of the Few-Layer Graphene. J Chem Phys C, 2009. 113: 16464-7.

5 Zhang, X., et al., Graphene nanoribbon band-gap expansion: Broken-bond-induced edge strain and quantum entrapment. Nanoscale, 2010. 2: 2160-3.

6 Sun, C.Q., S.Y. Fu, and Y.G. Nie, Dominance of Broken Bonds and Unpaired Nonbonding pi-Electrons in the Band Gap Expansion and Edge States Generation in Graphene Nanoribbons. J Chem Phys C, 2008. 112: 18927-34.

7 Sun, C.Q., Size dependence of nanostructures: Impact of bond order deficiency. Prog. Solid State Chem., 2007. 35: 1-159.

8 Sun, C.Q., Dominance of broken bonds and nonbonding electrons at the nanoscale. Nanoscale, 2010. 2: 1930-61.

### T7.2 Graphene Study: from fundamental to edge modification, intercalation and applications in energy storage (INVITED)

Zexiang Shen

Thursday, February 23, 04.30 PM, Lecture Theatre LT31

(TBA)

### T7.3 Investigation of graphene edge dynamics by using polarized Raman spectroscopy

Da Zhan, Zhenhua Ni, Jiaxu Yan, Lei Liu, Zexiang Shen

Thursday, February 23, 05.00 PM, Lecture Theatre LT31

The electronic properties of graphene nanoribbon are very sensitive to its edge structures. As the graphene edge structures are easy to be modified under thermal annealing, and thus the understanding of the thermal stability and dynamics of graphene edges are very important. It is found that edges of single layer graphene (both armchair and zigzag) are not stable and undergo modifications even at temperature as low as 200°C as the D band becomes activated. It is found that the Raman D band becomes activated and the intensity of 300°C annealed zigzag edge is comparable to that of armchair edge; this indicate the structurally modification during annealing. Furthermore, based on polarized Raman results, we provide structure evolution models of graphene edges during annealing. The zigzag edges rearrange and form armchair segments that are $\pm 30°$ relative to the edge direction, while armchair edges are dominated by armchair segments even at annealing temperature as high as 500°C. In contrast to the thermally unstable edges of single layer graphene, it is found that the AB-stacked bi-layer graphene perform obviously different thermal dynamics behavior, particularly that the zigzag edges of bi-layer graphene do not present any activated D band after annealing. The absence of activation of D band for such annealed bi-layer graphene zigzag edges indicates that the edges transform to closed state. The possibility of such structure transformation has also been supported by theoretical calculation results as the closed zigzag edges of AB-stacked bi-layer graphene present both compatible geometry and favorable energy. The studies of edge dynamics for single and bi-layer graphene are very useful for effectively controlling electronic properties of graphene nanostructures.

### T7.4 Superior Optical Limiting Observed in Functionalized graphene nanocompostes

Tingchao He, Handong Sun

Thursday, February 23, 05.15 PM, Lecture Theatre LT31

The increased utilization of high power laser sources has rendered great challenges for designing efficient optical limiting (OL) materials to protect human eyes and various delicate optical devices. An ideal optical limiter should greatly attenuate intense laser beam while exhibiting high transmittance for low input optical intensity. In the report, we will present the superior OL effects observed from two novel graphene oxide (GO) based nanocomposites. One is the nanocomposite made of graphene oxide (GO) and upconversion rare earth nanoparticles (NaYF4:Yb3+/Er3+). This novel material can dramatically improve OL performance of GO and broaden the working frequencies and wavelengths of lasers into the femtosecond pulse domain and the near-infrared regime. The other one is the noncovalently functionalized amphiphilic graphene composite. Our experimental results, for the first time, show that this nanocomposite in both polar and nonpolar solvents and its thin solid film display broadband OL response, indicating that the noncovalently functionalized amphiphilic graphene nanocomposite is an effective alternative to the covalently functionalized graphene hybrid materials. The nonlinear optical mechanisms observed in nanomaterials, i.e. nonlinear scattering, two-photon absorption, thermal lensing effect and energy transfer, are discussed in conjunction with the influence of the materials properties and laser source on the OL performance.

## 6.7 T8 Atomic & Optical Physics

This session on "Atomic & Optical Physics" will be held on Thursday, February 23, from 04.00 PM to 05.30 PM. The venue for this session is Seminar Room 03-07. Time allocated for invited talks is 25 min speaking time, plus 5 min questions, and time allocated for contributed talks is 12 min speaking time plus 3 minutes questions.

### T8.1 Superconducting Atom Chip

Chan Kin Sung, Sierke Mirco, Mussie Beian

Thursday, February 23, 04.00 PM, Seminar Room 03-07

An atom chip is a device where micrometer and nanometer microstructures can be fabricated, designed and engineered to manipulate, interfere and transport atomic quantum systems in a versatile manner. In recent years, there has been a growth of interest in using superconductors rather than normal conductors in atom chips due to the absence of thermal noise. This results in long decoherence times, which is important in quantum information processing. Our group has demonstrated the use of a type-II superconductor-YBCO as a magnetic trap for ultracold atoms. Persistent vortex currents in the YBCO are programmed with external magnetic fields, such that different configurations of magnetic traps are achieved. Our studies serve as an important step towards the interfacing of superconducting device and ultracold atoms.

### T8.2 Atomic excitation with propagating light pulse and quantum memory with a half cavity

Jiri Minar, Yimin Wang, Valerio Scarani

Thursday, February 23, 04.15 PM, Seminar Room 03-07

State mapping between atoms and photons and photon-photon interactions play a key role in scalable quantum information processing. First, we consider the interaction of a single atom with a quantized light pulse propagating in free space. We show the dependence of the atomic excitation on the quantum state of the pulse. We present a detailed study for both n-photon Fock state and coherent state pulses with various temporal shapes. Secondly, we propose a setup for quantum memory based on a single two-level atom in a half cavity with a moving mirror. We show that various temporal shapes of incident photon can be efficiently stored and readout by shaping the time-dependent decay rate $\gamma(t)$ describing the interaction between the atom and the light. We present an analytical expression for the efficiency of the storage and study its dependence on the ratio between the incident light field bandwidth and the atomic decay rate. We discuss possible implementations and experimental issues, particularly for a single atom or ion in a half cavity as well as a superconducting qubit in the circuit QED.

### T8.3 Dimensional Crossover in Bose-Hubbard model

Zhifeng Zhang, Pinaki Sengupta

Thursday, February 23, 04.30 PM, Seminar Room 03-07

Dimensionality plays an important role in condensed matter physics. The 3-D Bose-Hubbard model has Bose-Einstein Condensate as its ground state with a finite critical temperature. As the interlayer coupling is weakened, the critical temperature is suppressed. When the interlayer coupling decreases below a critical point, the system starts to have the behavior of a 2-D Bose-Hubbard model. The quasi-2-D system will enter the Berezinsky-Kosterlitz-Thouless (BKT) phase before it comes to the BEC ground state. In this talk, I will present the result of our Quantum Monte Carlo study which revealed this dimensional crossover phenomenon.

### T8.4 Towards a portable atom gravimeter

J. S. Raaj Vellore Winfred, Andrew Chew, Maral Sahelgozin, Yon Mingli, Ley Yuan, Rainer Dumke

Thursday, February 23, 04.45 PM, Seminar Room 03-07

Recent advancements in gravimeter based on atom interferometry has enabled measurement of gravity with high accuracy and precision. A portable atom gravimeter would allow measurement of gravity in various environments in situ. Such precise measurement of gravity is very important in technological and scientific endeavors. In this talk, an outline of different types of gravimeters and their performance will be highlighted. I will present an overview of our portable atom gravimeter experiment.

### T8.5 Excitation of a single atom with a temporaly shaped light pulses

Syed Abdullah Aljunid, Dao Hoang Lan, Gleb Maslennikov, Yimin Wang, Valerio Scarani, Christian Kurtsiefer

Thursday, February 23, 05.00 PM, Seminar Room 03-07

We investigate the interaction between a single atom and coherent optical pulses with a controlled temporal envelope. By switching the temporal shape from rising exponential to square profile, we show that the rising exponential envelope leads to higher excitation probability using lower photon number in a pulse. The atomic transition saturates for $\approx$ 100 photons in a pulse. Rabi oscillations with 100 MHz frequency are visible in detected fluorescence for excitations powers of $\approx$ 1300 photons in a 15 ns pulse. A possibility to excite the atom with pulses in a Fock states is discussed and the theoretical treatment is presented.

[1] Yimin Wang et al., Phys. Rev. A. **83** 063842 (2011)
[2] M. Stobińska et al., EPL **86** 14007 (2009)
[3] I. Gerhardt et al., Phys. Rev. A **79** 011402(R) (2009)

### T8.6 Measuring quantum correlations using lossy photon-number-resolving detectors with Saturation

Si Hui Tan, Leonid Krivitsky, Berge Englert

Thursday, February 23, 05.15 PM, Seminar Room 03-07

The variance of difference is an established measure of quantum correlation in quantum states of light. It allows us to discriminate between the classical correlation of a two-mode coherent state and the quantum correlation of a twin-beam state. It has already been shown that with losses, the variance of difference remains a good measure of quantum correlations in the twin-beam state and is an easy-to calculate function of quantum efficiency. The measurement of a normalized form of the variance of difference of the twin-beam state is thus used in experiments to calibrate the quantum efficiency of photodetectors. Here, the effect of saturation in the photodetector on its measurement of the variance of difference is investigated. It is found that the variance of difference is no longer a reliable entanglement measure at saturation of the detector but it remains useful in some range of average photon number of the incident light. A way to calibrate saturating photo detectors under the assumption that loss and saturation are small perturbations in the photocouunts is also presented.

## 6.8 T9 Energy & Materials

This session on "Energy & Materials" will be held on Thursday, February 23, from 04.00 PM to 05.15 PM. The venue for this session is Seminar Room 03-04. Time allocated for invited talks is 25 min speaking time, plus 5 min questions, and time allocated for contributed talks is 12 min speaking time plus 3 minutes questions.

### T9.1 Recent advances in energy storage materials (INVITED)

M V Reddy Reddy, B V R Chowdari

Thursday, February 23, 04.00 PM, Seminar Room 03-04

The rechargeable lithium ion batteries (LIBs) are the present-day choice for use in portable electronic appliances (mobile phones, digital cameras, i-pod and note-book computers) and very recently, they are being put use in hybrid vehicles as power sources. The LIBs consist of layer-type material such as LiCoO2 as the cathode (positive) and graphite as anode (negative)) and lithium (Li)-ion containing polymeric gel or non-aqueous solution as the electrolyte. The Li-ions intercalate in to the graphite and de-intercalate from the LiCoO2 during the charging operation and thus, store the electrical energy in the form of chemical energy. During discharge, the reverse reaction occurs. LIBs possess good working-voltage (3.6V) and high energy-density ( 200 Wh/kg; 300 Wh/l) compared to the other rechargeable batteries like Ni-Cd, Ni-MH and Pb-acid batteries. At present, annual production of LIBs is worth about USD 6 billion. Industry-projected demand and growth is 30-40% per year for the next 10 years with a market value exceeding USD10 billion. Recently many research groups (Physicists, Chemists and Materials Scientists) all over the world are working in the area of LIBs to search for novel electrode and electrolyte materials and optimize the known materials to reduce the cost, improve the performance and operational safety. Further, basic researches on electrode materials are needed to understand the physical, chemical and electrochemical properties of the materials In my talk, I will discuss principles operation of LIBs, recent advances on cathode, anode and electrolyte materials for LIBs. It includes preparation of simple and complex oxides by molten salt method, carbothermal reduction method, hydrothermal, sol-gel, ball-milling method etc. Materials characterization by Rietveld refinement X-ray diffraction, Neutron diffraction, X-ray absorption spectroscopy (XAS), X-ray photoelectron spectroscopy (XPS), SEM, TEM, density and BET surface area methods, and cyclic voltammetry, galvanostatic cycling and Insitu studies like electrochemical impedance spectroscopy and neutron diffraction techniques. At end I will discuss our group studies on asymmetric supercapacitor and solar cell performance of selected compounds.

### T9.2 Nanocrystals for thermoelectric energy conversion (INVITED)

Qingyu Yan

Thursday, February 23, 04.30 PM, Seminar Room 03-04

Low dimensional thermoelectric semiconductors are attractive as they are predicted to show improved efficiency as evaluated by the figure of merit ZT through increasing the seebeck coefficient and decreasing thermal conductivity. Enhanced seebeck coefficient has been demonstrated in thermoelectric nanoparticle assembly but with a low charge carrier concentration and electrical conductivity, which cannot lead to increased ZT values. Controlled doping of semiconductor nanocrystals is not easy as debatable issues related to the 'self-purification' process. Here, we will summarize our research work on developing high efficiency thermoelectric nanocrystals and some of the key issues. Also, we will discuss about the development of low-cost flexible thermoelectric films using carbon nanotubes and graphenes.

### T9.3 Metal Oxide/Cadmium Chalcogenide Composite nanostructures for photoelectrochemical hydrogen evolution

Jingshan Luo, Hongjin Fan

Thursday, February 23, 05.00 PM, Seminar Room 03-04

Hydrogen is the simplest form of chemical fuel which can be produced from splitting the water using sunlight. It thus represents one of the clean energy sources. A device that could directly harvest the energy from the sunlight and split the water into hydrogen, the so-called artificial leaf, is receiving wide research attention. TiO2 is a commonly used material in photoelectrochemical hydrogen evolution due to its high photoactivity, low cost and excellent chemical stability. However, the absorption of the sunlight is limited to the UV regime due to its large band gap (3.2 eV). Hence they are generally coated with narrow-bandgap semiconductors as the sensitizer. Here, we sensitize TiO2 nanorods, which are grown by chemical vapour deposition, with CdS, CdSe and their alloy which could absorb the visible part of the sunlight. When constructed into a photoelectrochemical cell with hole-scavenging electrolyte, the photocurrents are measured and compared. All samples show evident enhancement in photocurrent, which are compared with respect to their light absorption. By measuring the transient photocurrents, information on the stability of the three different samples can be indicated. In trade of the performance and stability, we propose that the CdSeS alloy sensitized sample is the best.

## 6.9 T10 Biophysics

This session on "Biophysics" will be held on Friday, February 24, from 09.00 AM to 10.30 AM. The venue for this session is Lecture Theatre LT31. Time allocated for invited talks is 25 min speaking time, plus 5 min questions, and time allocated for contributed talks is 12 min speaking time plus 3 minutes questions.

### T10.1 Probing nano-materials and bio-materials with holographic video microscopy (INVITED)

Fook Chiong Cheonbg

Friday, February 24, 09.00 AM, Lecture Theatre LT31

Coherent light scattered by individual colloidal particles carries comprehensive information on each particle's shape, size, three-dimensional position and composition. New advances in holographic video microscopy enable us to track individual colloids with nanometer-scale resolution over ranges of hundreds of micrometers, and simultaneously to characterize each particle's optical properties with part-per-thousand precision, all with video-rate time resolution. The ready availability of precise, time-resolved and particle-resolved data creates new opportunities for research in a host of fields ranging from bio- and statistical physics to medical diagnostics and drug discovery.

### T10.2 Measurement of Photon Statistics with Live Photoreceptor Cells

Leonid Krivitsky, Nigel Sim, Mei Fun Cheng, Mike Jones, Dmitry Bessarab

Friday, February 24, 09.30 AM, Lecture Theatre LT31

We analyzed the electrophysiological response of an isolated rod photoreceptor of *Xenopus laevis* under stimulation by coherent and pseudo-thermal light sources. Using the suction electrode technique for single cell recordings and a fiber optics setup for light delivery allowed measurements of the major statistical characteristics of the rod response. The results indicate differences in average responses of rod cells to coherent and pseudo-thermal light of the same intensity and also differences in signal-to-noise ratios and second order intensity correlation functions. These findings should be relevant for interdisciplinary studies in applications of quantum optics in biology.

### T10.3 Yield strain of human erythrocytes membrane to impulsive stretching

Fenfang Li, Claus Dieter Ohl, Chon U Chan

Friday, February 24, 09.45 AM, Lecture Theatre LT31

The deformability of cells without its rupture is an important mechanical property. In particular red blood cells need to deform considerably while flowing through small capillaries. It has been confirmed that the RBC membrane can withstand a finite strain, beyond which it ruptures. The classical and very small yield areal strain of 2-4% for RBCs has been measured using micropipette aspiration by Evans et al in 1976. However, Leverett et al noted already in 1972 that this threshold is a function of the exposure duration, and may increase dramatically for shorter durations of the forcing. Here, we quantify the yield strain for RBC membrane rupture using an impulse like forcing. Therefore, a collection of RBCs are stretched by the fast and transient flow created by a single laser-induced cavitation bubble. The duration of the fluid flow is in the tens of microseconds. The deformation of the cells is captured by a high speed camera and viability is monitored with fluorescence microscopy successively. We find that the probability of cell survival is closely related to the initial strain. Yet, the threshold linear and areal strain for membrane failure is much larger as compared to micropipette aspiration. Membrane integrity is assessed from the diffusion of fluorophores through the plasma membrane.

### T10.4 Deterministic Rogue Waves (INVITED)

Jorge Tredicce

Friday, February 24, 10.00 AM, Lecture Theatre LT31

Rare extreme events can occur in many different systems in nature. A typical example is rogue waves observed in the oceans, where waves higher than 30 meters are more or less common phenomena. Scientist interest on extremely high waves increased substantially during the last decade not only in oceanographic studies but also in other systems such as capillary waves and optical waves. Both, from theoretical and experimental point of view there are several questions still remaining unsolved. The physical mechanisms that originate them , the way they develop, the probability for them to occur, the type of system able to generate such extreme events, and the connections between extreme events in systems which are apparently completely different, are being the subjects of intensive research. The understanding of the generation of rare extreme events it is interesting for itself, but also can allow identifying mechanisms to control or suppress the occurrence of such events. In this way, the investigation of the phenomenon in a controllable experimental setup is very important from a practical point of view and offers a great possibility to shade new light in this subject.

In this work we investigate, both theoretically and experimentally, the appearance of rare giant pulses or "optical rogue waves" in a semiconductor laser subject to optical injection and a mode locked Ti:Sa laser. We perform a detailed experimental characterization of the parameter region where rogue waves appear, and compare the experimental observations with numerical results. It is shown that the sporadic large intensity events can be understood as a result of a *deterministic nonlinear process*.

## 6.10 T11 Optical Characterization of Condensed Matter

This session on "Optical Characterization of Condensed Matter" will be held on Friday, February 24, from 09.00 AM to 10.30 AM. The venue for this session is Seminar Room 03-07. Time allocated for invited talks is 25 min speaking time, plus 5 min questions, and time allocated for contributed talks is 12 min speaking time plus 3 minutes questions.

### T11.1 Ultrafast Optical Spectroscopy of Semiconducting Nanostructures (INVITED)

Tze Chien Sum

Friday, February 24, 09.00 AM, Seminar Room 03-07

Ultrafast optical spectroscopy techniques (e.g. time resolved photoluminescence (TR-PL) and transient absorption (TA) spectroscopy) are very powerful probes to investigate the charge carrier dynamics in semiconducting nanostructures. Herein, we showcase some of our latest work on the study of carrier dynamics in Cu-doped ZnO nanowires and CdSe nanodot/ CdS nanorod heterostructures:

Cu-doped ZnO Nanowires Both TR-PL and TA reveal an ultrafast charge transfer (CT) process, with an electron localization time constant , between the ZnO host and the Cu dopants in Cu-doped ZnO nanowires. This CT process effectively competes with the ZnO band edge emission, resulting in the quenching of the ZnO UV emission. TR-PL measurements show that the UV decay dynamics coincides with the build-up of the Cu-related green emission. TA measurements probing the state-filling of the band edge and defect states provide further support to the CT model where the bleaching dynamics concur with the TR-PL lifetimes

CdSe nanodot/ CdS nanorod heterostructures CdSe seed CdS nanorod heterostructures is a fine example of seeded nanorod heterostructures comprising of a nanodot imposing 3D confinement with fully quantized states and a rod-shaped shell exhibiting quasi 1-D confinement. In this system, the CdSe core is located closer to one end of the rod (along $\frac{1}{4}$ of its total length) rather than its center due to higher reactivity of the facet over the facet. Such systems of mixed dimensionality provide an interesting platform for many fundamental optical and electronic studies. High quality samples with quantum yields (reaching 70%) have been fabricated. Time-resolved optical spectroscopy showed that suppressed Auger processes can lead to the realization of amplified spontaneous emission in these samples.

### T11.2 New experimental methods: ultraviolet-vacuum ultraviolet magneto-optical ellipsometry and resonant soft X-ray scattering on strongly correlated electron and biological systems (INVITED)

Andrivo Rusydi

Friday, February 24, 09.30 AM, Seminar Room 03-07

(TBA)

### T11.3 Raman studies on thickness-dependent doping in mono-and few-layer graphene

Namphung Peimyoo, Ting Yu, Jingzhi Shang, Chunxiao Cong, Huanping Yang

Friday, February 24, 10.00 AM, Seminar Room 03-07

Here we report doping effects on exfoliated mono-, bi-, tri- and tetralayer graphene induced by methy orange (MO). Charge transfer between graphene and MO caused two outcomes simultaneously. One is the strong chemical doping in graphene layers and the other is the enhancement of molecular Raman signals. The systematic Raman mapping and spectroscopy analysis clearly reveal thickness dependence of doping effects and enhanced Raman signals of MO. The doping level is found to be highest in monolayer graphene and decreases with the number of graphene layers. The possible origins of thickness-dependence of doping effect were discussed and designated to the different band structures of graphenes and the screening effect. Our finding provides a potential approach for modifying the electronic properties of graphene layers and investigating the vibrational properties of molecules.

### T11.4 Quasiparticle dynamics in overdoped Bi1.4Pb0.7Sr1.9CaCu2O8+δ: Coexistence of superconducting gap and pseudogap below Tc

Saritha K. Nair, Xingquan Zou, Jian-Xin Zhu, Christos Panagopoulos, Shigeyuki Ishida, Shin-Ichi Uchida, Elbert E.M. Chia

Friday, February 24, 10.15 AM, Seminar Room 03-07

Photoexcited quasiparticle relaxation dynamics in overdoped Bi2Sr2CaCu2O8+δ (Tc=65 K, hole doping p=0.22) single crystal is investigated as a function of temperature. We provide evidence of a $\sim$22 meV pseudogap (T$*\approx$100 K) at this doping level. Moreover, this pseudogap vanishes at T$*$. Our data support the scenario where both the superconducting gap and pseudogap coexist in the superconducting state. Our results also suggest an increased scattering rate between electrons and spin fluctuations as the sample enters the pseudogap phase.

## 6.11 T12 Semiconductors

This session on "Semiconductors" will be held on Friday, February 24, from 09.00 AM to 10.15 AM. The venue for this session is Seminar Room 03-04. Time allocated for invited talks is 25 min speaking time, plus 5 min questions, and time allocated for contributed talks is 12 min speaking time plus 3 minutes questions.

### T12.1 Band structure of multilayer dilute nitride semiconductor (INVITED)

W. J. Fan

Friday, February 24, 09.00 AM, Seminar Room 03-04

An universal 10-band k.p formula for arbitary multilayer semiconductors including dilute nitride semiconductors are derived, which can be used to calculate not only the 10-band k.p band structure but the 8- and 6-band k.p band structures also. In this work, the band structures of AlGaAs/GaAs/AlGaAs three layers (quantum well) are calculated using the 10-band k.p formula and compared with the 8-band k.p results, and found they are in very good agreement. The 10-band k.p band structures of GaAsN/InGaAsN/GaAsN quantum well are obtained. Spurious solutions are checked, we did not found the spurious solutions at our concerned energy and wavevector ranges.

### T12.2 Optical anisotropy of III-V nanowires

Christophe Wilhelm, Alexandre Larrue, Xing Dai, Sen Zhang, Dmitri Migas, Cesare Soci

Friday, February 24, 09.30 AM, Seminar Room 03-04

Semiconductor nanowires of the III-V group present several advantages in terms of opto-electronic properties that place them as good candidates toward the development of future nanometer scale devices. Whereas the advances of bottom-up growth techniques has lead to the synthesis of purely single phase nanowires in either zinc blende or wurtzite crystalline structure, the origin of the anisotropy in their optical properties is still not completely unraveled. The main sources of anisotropy stem from the intrinsic properties of the crystallographic structure of the nanowire combined with dielectric effects due to their high aspect ratio. A short review on the growth conditions necessary to obtain single phase nanowires will be first presented. The interband dipole transitions selection rules will be summarized for common III-V materials, and confirmed by ab initio Density Functional Theory calculations of the oscillator strength. Both the effect of the refractive index mismatch between the wire and it surrounding media and the polarization of the emitted light imposed by the crystalline structure will be discussed. Moreover, electromagnetic simulations of free standing nanowires have been conducted to study both the effect of the diameter, and the orientation of the excitation dipole on the radiation pattern of the nanowire in the far field. The importance of the correlation between optoelectronic properties and the crystalline structure is highlighted in view of potential nanowire-based optoelectronic applications, such as nanowire lasers.

### T12.3 Self-Assembly and Electrical Properties of GaAs Nanowire Junctions

Xing Dai, Shadi Dayeh, Nan Meng, Alexandre Larrue, Haibin Su, Cesare Soci

Friday, February 24, 09.45 AM, Seminar Room 03-04

The self-assembly of monolithic GaAs nanowire junctions by Metal-Organic Chemical Vapor Deposition is demonstrated. Formation of the junctions results from the fine balance between the electrostatic interaction of polar facets of III-V nanowires and the mechanical strength of two merging nanowires during metal nanoparticle assisted Vapor-Liquid-Solid growth. High resolution transmission electron microscopy reveals the nature and periodicity of the polar facets and the atomic structure of the junction. Electrostatic-mechanical modeling and position-controlled synthesis are used to understand the relationship between spontaneous junction formation and nanowire diameter, length, and inter-distance, and to formulate a universal model that accurately depicts such phenomenon in polar faceted semiconductor nanowires. Transport properties of three-terminal Y-junction devices are investigated by physics-based device simulations and electrical measurements, showing the potential of controlled self-assembly of monolithic junctions to realize large area integration of novel functional nanowire device concepts, such as nanowire intracellular probes and nanowire quantum junctions.

### T12.4 Germanium Surface Passivation by Direct Atomic Source Nitridation

Ming Yang, Yuanping Feng, Shijie Wang

Friday, February 24, 10.00 AM, Seminar Room 03-04

Surface passivation of Germanium surface is a very critical issue for fabricating high performance semiconductor devices and integrating heterogeneous materials with Germanium. Compared with conventional thermal nitridation process by using ammonia or dry oxygen gas, which should be performed at higher temperature and will incorporate large amounts of unstable defects on the surface of semiconductors, the atomic source nitridation and oxidation processes have advantages of lower temperature, higher dense, and no surface destruction, etc. In this talk, we present in-situ surface passivation for Germanium by using direct atomic source nitridation and oxidation. In-situ photoelectron spectroscopy (XPS) was used to study the high-temperature thermal stability and band alignments at dielectrics and Germanium interfaces. Combinational characterization by using TEM, XPS, AFM and STM with first-principles calculation was applied to study the dielectric and electronic properties of surface passivation layers. It shows that direct surface passivation by atomic source can produce high quality passivation layers with excellent electrical properties and high chemical stability, and can be used for variety of applications in semiconductor device fabrication and precise surface coating.

## 6.12 T13 Graphene II

This session on "Graphene II" will be held on Friday, February 24, from 11.00 AM to 12.15 PM. The venue for this session is Lecture Theatre LT31. Time allocated for invited talks is 25 min speaking time, plus 5 min questions, and time allocated for contributed talks is 12 min speaking time plus 3 minutes questions.

### T13.1 Two-Dimensional Semiconducting Nanosheets: Preparation, Characterization, Properties and Applications (INVITED)

Hua Zhang

Friday, February 24, 11.00 AM, Lecture Theatre LT31

In this talk, I will summarize the recent research on synthesis, characterization and applications of 2D semiconducting nanomaterials in my group [1]. I will introduce the synthesis and characterization of novel 2D semiconducting materials, such as graphene [2], MoS2, WS2, TiS2, TaS2, etc. [3], especially the first-time synthesized hexagonal-close packed (hcp) Au nanostructures on graphene oxide [4]. Then I will demonstrate the applications of the 2D nanomaterials in chemical and bio-sensors [5], solar cells [6], electric devices [7], memory devices [8], conductive electrodes [5b, 6a-b, 7-9], cell cultures [10], matrix of MALDI-TOF-MS [11], supercapacitors [12] etc.

[1] (a) X. Huang, et al., Chem. Soc. Rev., 2012, 41, 666. (b) X. Huang, et al., Small 2011, 7, 1876.

[2] (a) X. Y. Qi, et al., Angew. Chem. Int. Ed., 2010, 49, 9426. (b) X. Y. Qi, et al., Small, 2010, 6, 66369. (c) X. Huang, et al., Small, 2010, 6, 513. (d) X. Z. Zhou, et al., J. Phys. Chem. C, 2009, 113, 10842. (e) S. X. Wu, et al., Nanoscale, 2012, DOI:10.1039/C2NR11992G.

[3] (a) Zeng, Z. Y.; et al. Angew. Chem. Int. Ed. 2011, 50, 11093. (b) Li, H.; et al. Small 2012, 8, 63. (c) Yin, Z. Y.; et al. ACS Nano 2012, 6, 74. (d) Li, H.; et al. Small 2012, DOI: 10.1002/smll.201101958.

[4] (a) X. Huang, et al., Nat. Commun. 2011, 2, 292. (b) X. Huang, et al., Angew. Chem. Int. Ed. 2011, 50, 12245. (c) X. Huang, et al., Adv. Mater. 2012, 24, 979.

[5] (a) Q. Y. He, et al., ACS Nano, 2010, 4, 3201. (b) Q. Y. He, et al., ACS Nano, 2011, 5, 5038. (c) X. H. Cao, et al., Small, 2011, 7, 1199. (d) H. G. Sudibya, et al., ACS Nano, 2011, 5, 1990. (e) Z. J. Wang, et al., J. Phys. Chem. C, 2009, 113, 14071. (f) Z. J. Wang, et al., Biosens. Bioelectron., 2011, 26, 3881. (f) G. Lu, et al., Chem. Sci., 2011, 2, 1817. (g) Z. Y. Yin, et al. Nanoscale 2011, 4, 293.

[6] (a) Z. Y. Yin, et al., ACS Nano, 2010, 4, 5263. (b) Z. Y. Yin, et al., Small, 2010, 6, 307. (c) J. L. Song, et al. Chem. Eur. J., 2011, 17, 10832.

[7] B. Li, et al., Adv. Mater., 2010, 22, 3058. [8] (a) J. Q. Liu, et al., ACS Nano, 2010, 4, 3987. (b) J. Q. Liu, et al., Small, 2010, 6, 1536.

[9] (a) S. X. Wu, et al., J. Phys. Chem. C, 2010, 114, 11816. (b) S. X. Wu, et al., J. Mater. Chem., 2011, 21, 3467. (c) S. X. Wu, et al. J. Phys. Chem. C, 2011, 115, 15973.

[10] S. Agarwal, et al., Langmuir, 2010, 26, 2244.

[11] X. Z. Zhou, et al., Chem. Commun., 2010, 46, 6974.

[12] X. H. Cao, et al. Small, 2011, 7, 3163.

### T13.2 New understandings of Raman bands of graphene (INVITED)

Ting Yu

Friday, February 24, 11.30 AM, Lecture Theatre LT31

Graphene, as an exceptional two dimensional material possesses extremely promising potential for fundamental studies and practical applications. Here we report our recent study on the Raman bands of graphene. From the low frequency to the intermediate frequency range, several NEW modes have been observed and assigned. The well-known Raman bands like D and G' or 2D have been given new understandings. Through this talk, we show that Raman spectroscopy and imaging can be used as a quick and unambiguous method to determine the in-plane and out-of-plane arrangement of carbons in graphene layers. The results presented here are highly relevant to the application of graphene in nano-electronic devices and help in developing a better understanding of the physical and electronic properties of graphene.

### T13.3 Ultrafast carrier dynamics in pristine and FeCl3-intercalated bilayer graphene

Xingquan Zou, Da Zhan, Xiaofeng Fan, Dongwook Lee, Saritha K Nair, Sun Li, Zhenhua Ni, Zhiqiang Luo, Lei Liu, Ting Yu, Zexiang Shen, Elbert E. M. Chia

Friday, February 24, 12.00 PM, Lecture Theatre LT31

Ultrafast carrier dynamics of pristine bilayer graphene (BLG) and BLG intercalated with FeCl3 (FeCl3–G), were studied using time-resolved transient differential reflection (Delta R/R). Compared to BLG, the FeCl3–G data showed an opposite sign of Delta R/R, a slower rise time, and a single (instead of double) exponential relaxation. We attribute these differences in dynamics to the down-shifting in the Fermi level in FeCl3–G, as well as the formation of numerous horizontal bands arising from the d-orbitals of Fe. Our work shows that intercalation can dramatically change the electronic structure of graphene, and its associated carrier dynamics. (Applied Physics Letters 97, 141910 (2010))

## 6.13 T14 Photonic Devices/Astrophysics

This session on "Photonic Devices/Astrophysics" will be held on Friday, February 24, from 11.00 AM to 12.30 PM. The venue for this session is Seminar Room 03-07. Time allocated for invited talks is 25 min speaking time, plus 5 min questions, and time allocated for contributed talks is 12 min speaking time plus 3 minutes questions.

### T14.1 Spectroscopic characterization for photonics devices (INVITED)

Handong Sun

Friday, February 24, 11.00 AM, Seminar Room 03-07

In this talk I will present our recent progress in spectroscopic characterization on various photonic materials and the development of microlasers. 1. Photoluminescence characterization of dipole forbiden oxides; 2. Interaction between plasmonic structures and light emitting materials; 3. Nonlinear transmission of some nanostructured materials; 4 WGM based microlasers.

### T14.2 Enhancing the radiative properties of a semiconductor nanowire coupled to a photonic crystal microcavity (INVITED)

Alexandre Larrue, Christophe Wilhelm, Sen Zhang, Sylvain Combrie, Alfredo De Rossi, Cesare Soci

Friday, February 24, 11.30 AM, Seminar Room 03-07

A novel photonic structure formed by the hybrid integration of a vertical III-V nanowire on top of a two-dimensional photonic crystal microcavity is proposed to enhance light emission from the nanowire. The enhancement of spontaneous emission rate is described by a generalized Purcell factor, whereas the material gain at threshold is used as a figure of merit toward the design of a vertical emitting nanolaser. Depending on nanowire radius, two coupling regimes with a L3 photonic crystal microcavity are identified by Finite-Difference-Time-Domain simulations. Ultra-thin nanowires evanescently coupled to the microcavity lead to greater enhancement of the spontaneous emission rate, while nanowires with large radii provide better overlap with the active gain medium but overall lower Purcell factors. A trade-off is identified for a nanowire radius of r=0.2 a and length L=a. Modification of the directivity of the L3 photonic crystal cavity based on the folding principle is employed to further optimize the far-field radiation pattern and increase the overall directivity of the hybrid structure, demonstrating the feasibility of this approach toward large scale integration of single mode vertical nanolasers and intra-chip optical interconnects.

### T14.3 Flexible Microlaser

Rui Chen, Van Duong Ta, Handong Sun

Friday, February 24, 12.00 PM, Seminar Room 03-07

At present, investigation on optical microresonators have attracted extensive research interest due to their small mode volume and high quality factor for fundamental physics investigation, and attractive applications in lasers, active filters and sensing devices. In this talk, we present our recent work about three-dimensional confined flexible microresonator combining self-assembled dome-shape microstructure with a planar Bragg reflector. By incorporating dye molecules into the microstructure, optically pumped whispery gallery mode lasing phenomenon is observed at room temperature. Studies about the lasing behaviors with different cavity sizes, and particularly single longitudinal mode lasing will be discussed. Moreover, polarization and lasing characteristics such as frequency shift and mode hopping will be presented. Owing to the flexibility and controllability, this work provides a excellent platform future investigation about light and matter interaction and spectacular new devices.

### T14.4 Galaxy Zoo - Dust lane early-type galaxies are tracers of recent, gas-rich minor mergers

Yuan-Sen Ting

Friday, February 24, 12.15 PM, Seminar Room 03-07

I am going to present the study of early-type galaxies (ETGs) with prominent dust lanes. Two thirds of these 'dusty ETGs' (D-ETGs) (about 400 galaxies) are found to be morphologically disturbed which suggests a merger origin, making these galaxies ideal testbeds for studying the merger process at low redshift. We illustrated that D-ETGs exhibit bluer UV-optical colours indicating enhanced levels of star formation and an AGN fraction compare to their normal ETGs counterparts, indicating strikingly higher levels of nuclear activity. We used optical and radio data to examine the nature of AGN activity in these objects. Our results have indicated that D-ETGs represent an evolutionary stage between starbursting and quiescent galaxies. In these objects, the AGN has already been triggered but has not yet completely destroyed the gas reservoir required for star formation.

## 6.14 T15 Carbon Nanotubes/Physics of Continua

This session on "Carbon Nanotubes/Physics of Continua" will be held on Friday, February 24, from 11.00 AM to 12.30 PM. The venue for this session is Seminar Room 03-04. Time allocated for invited talks is 25 min speaking time, plus 5 min questions, and time allocated for contributed talks is 12 min speaking time plus 3 minutes questions.

### T15.1 Dichlorocarbene Functionalization of Single Walled Carbon Nanotubes (INVITED)

Qing Zhang, Chao Liu

Friday, February 24, 11.00 AM, Seminar Room 03-04

In this talk, we shall present our recent progress in the effects of carbene-based covalent functionalization on the electrical properties of an isolated m-SWCNT, a semiconducting (s)-SWCNT, and a mixture network of both m- and s-SWCNTs are reported.[1] Upon dichlorocarbene functionalization, a semiconducting SWCNT is found to transfer to metallic SWCNT. The transition is reversible upon thermal annealing under ambient conditions. The electrical properties of m-SWCNTs remain largely unaffected whereas the on-state conductivity of s-SWCNTs is greatly reduced by this process, in agreement with the relevant theoretical predictions. Our findings can serve as important experimental evidence for a theoretical prediction: the covalent attachment of dichlorocarbene breaks sidewall C-C bonds of m-SWCNTs, leading to retention of two sp2 carbon bonding characteristics rather than formation of two sp3 rehybridization bonds for small diameter SWCNTs. [1] Chao Liu et al, SMALL 7(2011)1257

### T15.2 Directed Crystallization of CuSO4 3 5H2O onto Carbon Nanotube 2 Microarchitectures

Sharon Xiaodai Lim, Chornghaur Sow

Friday, February 24, 11.30 AM, Seminar Room 03-04

An assembly technique based on crystallization of thin CuSO4.5H2O microcrystals from salt solution onto patterned three-dimensional (3D) multiwalled carbon nanotube (MWNT) platform was developed. The vertically aligned MWNT arrays served as nucleation sites for the formation of microstructured CuSO4.5H2O crystals. In the presence of MWNTs, the CuSO4.5H2O crystal exhibited preferential crystallization in the (222) orientation. Sculpting theMWNT platforms using a focused laser beam, as well as utilizing capillary forces that occurred during the drying process of the salt solution, a variety of 3D MWNT-microcrystal hybrid systems were created. In addition to the 3D MWNT platform created by focused laser beam pruning, we have also achieved assembly of the microcrystals onto MWNT array with patterned hydrophilic and hydrophobic regions. Such chemical modifications of the MWNT surface were achieved without introducing any physical destruction to theMWNTarrays. As such, two-dimensional template-directed assembly of crystals onto the hydrophilic regions on the MWNT surface was realized.

### T15.3 High Energy Density Pulsed Plasmas: Novel Tool for Plasma Nanoscience

Rajdeep Singh Rawat

Friday, February 24, 11.45 AM, Seminar Room 03-04

This paper will review the applications of pulsed high energy density pinch plasmas, accompanied by instability accelerated energetic ion beams, from a dense plasma device in nanophase material synthesis. The plasma focus device, a coaxial plasma gun, being a multiple radiation source of ions, electron, soft and hard x-rays, and neutrons, has routinely been used for several applications such as lithography, radiography, imaging, activation analysis, radioisotopes production etc. This review paper highlights and critically discusses the key features of plasma focus device to understand the novelties and opportunities that this device can offer in plasma nanoscience. The results of recent key experimental investigations performed on the modification of various physical properties of PLD grown thin films of FePt, polymeric polyaniline thin film, zirconium solid substrate etc by energetic ion exposure in plasma focus device and the deposition of nanostructured FeCo, FePt, CoPt, ZnO, TiC etc thin films in plasma focus device will be reviewed.

### T15.4 Beryllium Activation Neutron Detection

Alireza Talebitaher, Stuart V. Springham, Paul Lee, Rajdeep S. Rawat

Friday, February 24, 12.00 PM, Seminar Room 03-04

Compact fast neutron detectors based on beryllium activation have been constructed to perform accurate DD fusion product neutron yield measurements on pulsed fusion devices. The detector comprises a beryllium metal sheet sandwiched between two large-area xenon-filled proportional counters. By comparison with other neutron detectors, our newly developed beryllium detector has advantages of: high sensitivity to 2.5 MeV DD fusion neutrons, short decay time, insensitivity to room-scattered neutrons, and high signal-to-background ratio. Moreover as the beryllium detector responds only to the fast neutrons, a moderator is redundant, making the detector very compact and able to be positioned close to the source. Energy calibration of the proportional counters using x-ray sources, along with numerical simulations performed using MCNP have been used to determine the absolute efficiency, or response factor, of the beryllium detector as a function of neutron energy. NX2 plasma focus device has been employed as a pulsed neutron source to test this new detector.

### T15.5 Hydrogen bond relaxation dynamics and the associated anomalies of ice

Xi Zhang, Chang Q Sun

Friday, February 24, 12.15 PM, Seminar Room 03-04

Coulomb repulsion between the unevenly-bounded bonding "-" and nonbonding ":" electron pairs in the "O2- : H+/p-O2-" hydrogen-bond is shown to originate the anomalies of low-compressibility, phonon relaxation dynamics, proton symmetrization in the hydrogen-bond, and the depression of the critical temperature for the VIII-VII phase transition of ice under compression. Consistency between molecular dynamics calculations and experimental observations confirmed our hypothesis that the resultant force of the compression, the repulsion, and the distortion of the unevenly-bonded electron pairs make the longer-and-softer intermolecular "O2- : H+/p" nonbonding lone pair highly compressed and stiffened but the shorter-and-stiffer intramolecular "H+/p-O2-" real bond elongated and softened. Consequently, softer nonbond phonons (¡ 400 cm-1) shift to lower frequency and the stiffer bond phonons (¿ 3000 cm-1) shift to higher frequency upon compression. The nonbond compression and the real bond elongation results in the O2–H+/p : O2- symmetrization and the low compressibility of ice. The cohesive energy of the real bond dominates the critical temperature of phase transition. Findings should form the starting point to unveil the physical anomalies of H2O under various stimuli.

1 Hydrogen bond relaxation dynamics and the associated anomalies of frozen H2O under compression, http://arxiv. org/abs/1110. 0075

2 Hydrogen bond relaxation dynamics and the associated vibronic and volumetric anomalies of H2O upon frozen, http://arxiv. org/abs/1109. 3958

## 6.15 T16 Novel Optical Materials

This session on "Novel Optical Materials" will be held on Friday, February 24, from 02.00 PM to 03.30 PM. The venue for this session is Lecture Theatre LT31. Time allocated for invited talks is 25 min speaking time, plus 5 min questions, and time allocated for contributed talks is 12 min speaking time plus 3 minutes questions.

### T16.1 A Tunable Nano/Micromachined Metamaterials (INVITED)

Weiming Zhu, Ai Qun Liu

Friday, February 24, 02.00 PM, Lecture Theatre LT31

Metamaterials are functional materials with rational designed sub-wavelength structures which may leads to unique EM properties such as negative refractive index, perfect absorption, sub-wavelength focusing and extraordinary transmission etc. Recently, tunable Nanomicromachined metamaterials based on MEMS fabrication technology is a new approach and the essential in applications where functional materials with designable electromagnetic (EM) properties and tunablilities are required, such as variable wave plates, tunable filters, optical delay line and controllable luminescence etc. Most of the existing tuning methods of the metamaterials are based on the nonlinearity of their construction materials or surrounding mediums which, somehow, limit the tunable capabilities of the metamaterials.

In this paper, it is to focus on new innovation of reconfigurable nano/micromachined metamaterials through tuning of unit cell microstructures. This novel approach for reconfigurable metamaterials not only enables large tuning range of the metamaterials but also shows the capabilities in tuning the metamaterials properties, which promises unique tunabilities on optical anisotropy, subwavelength resonance and focusing, light luminescence and optical activity etc.

[1] W. M. Zhu, A. Q. Liu, X. M. Zhang, D. P. Tsai, T. Bourouina, J. H. Teng, X. H. Zhang, H. C. Guo, H. Tanoto, T. Mei, G. Q. Lo and D. L. Kwong, "Switchable Magnetic Metamaterials Using Micromachining Processes," Advanced Materials, Vol 23, Issue 15, 2011.

[2] Y. H. Fu, A. Q. Liu, W. M. Zhu, X. M. Zhang, D. P. Tsai, J. B. Zhang, T. Mei, J. F. Tao, H. C. Guo, X. H. Zhang, J. H. Teng, N. I. Zheludev, G. Q. Lo, and D. L. Kwong, "A micromachined reconfigurable metamaterial via reconfiguration of asymmetric split-ring resonators," Advanced Functional Materials, Vol 21, Issue 18, 2011.

[3] W. M. Zhu, A. Q. Liu, W. Zhang, J. F. Tao, T. Bourouina, J. H. Teng, X. H. Zhang, Q. Y. Wu, H. Tanoto, H. C. Guo, G. Q. Lo and D. L. Kwong, "Polarization dependent state to polarization independent state change in THz metamaterials", Applied Physics Letters, Vol 99, 221102, 2011.

[4] W. M. Zhu, A. Q. Liu, T. Bourouina, D. P. Tsai, J. H. Teng, X. H. Zhang, G. Q. Lo, D. L. Kwong and N. I. Zheludev, "Tunable terahertz anisotropy", Nature Communications, submitted.

### T16.2 Tunable Subwavelength Terahertz Plasmonic Stub Waveguide Filters

Jin Tao, Qijie Wang

Friday, February 24, 02.30 PM, Lecture Theatre LT31

Tunable subwavelength terahertz (THz) plasmonic stub waveguide filters based on indium antimonide (InSb) are proposed and numerically investigated for the first time. The transmission line theory and the Finite Different Time Domain simulation results reveal that the single-stub waveguide structure can realize a stop-band filtering function and the central wavelength of the notch is linearly dependent on the stub length while nonlinearly dependent on the stub width. The central wavelength of the notch can be actively controlled by tuning the temperature. As an extension to the single-stub structure, multiple-stub InSb slot waveguide structures are also proposed and used to realize a wide stop-band filtering function. The proposed filters may have applications in THz highly-integrated plasmonic circuits.

### T16.3 Plasmonic Waveguide Platform for Electronic-photonic Integrated Circuits

Ping Bai, Hong Son Chu, Shiyang Zhu, Erping Li

Friday, February 24, 02.45 PM, Lecture Theatre LT31

Plasmonics relies on the propagation of electromagnetic waves along a metal-dielectric interface yielding strong mode confinement while seamlessly interfacing photonics and electronics. Its credentials to drive next-generation optical interconnect into new performance metrics have led to intense research during past years for bringing plasmonics from proof-of-concept demonstrations into system-qualified device development. Thus the plasmonics for optical interconnects will be a promising technology platform towards enabling the deployment of small-footprint and low-energy integrated circuitry, holding a great application for chip-scale and high integration density optical interconnects. In this talk, I will present the latest progress in IHPC on plasmonics for optic data transmission in electronic integrated circuits. Specifically, a novel plasmonic waveguide platform Cu/SiO2/Si/SiO2/Cu to build high-performance CMOS-compatible plasmonic devices for electronic-photonic integrated circuits will be presented. The platform is based on metal-silica-silicon hybrid plasmonic waveguides. The optical performance of the waveguide platform is investigated and analyzed extensively with various geometries both theoretically and experimentally. The propagation loss can be achieved as low as 0.4 dB/micrometer with a small SiO2/Si/SiO2 cross section of $100\times340$ square nm. The proposed waveguide platform can be used as an ideal building block to facilitate various plasmonic devices such as filters, splitters, multiplexes and modulators. As an example, a plasmonic ring resonator with the ring radius of 0.91 micrometer is designed with the platform. Excellent optical performance is measured including a free spectral range of 130 nm, extinction ratio of 24 dB, and insertion loss of 2.5 dB. Modulators, add-drop multiplexers and mode converters are to be developed with the proposed platform in the next step. We believe this work will bring one step further for the integration of nanoscale electronic-photonic integrated circuits.

### T16.4 Plasmonic Brillouin Scattering and filtering

Bing Wang, Yanjun Liu, Guangyuan Si, Eunice S. P. Leong, Ning Xiang, Aaron Danner, Jing Hua Teng

Friday, February 24, 03.00 PM, Lecture Theatre LT31

Plasmonics paves the way for manipulating optical signals at the nanoscale level by coupling light to coherent electronic excitations. The strong confinement of light associated with surface plasmon resonances has led to the development of various subwavelength photonic components. The conversion between photons and plasmons can be controlled at the subwavelength scale, which can make the plasmonic based device ultracompact. In this talk, we will report the manipulation of plasmonics in frequency domain and the application of plasmonics in wavelength filtering. Noble metallic annular aperture array (AAA), the plasmonic coaxial nanostructures, have the distinctive property of forming a Fabry-Pérot nanocavity to support plasmonic waveguide modes, which could lead to super-enhanced optical transmission with narrow pass bands. We will show here a AAA based wavelength filter at the visible range and the integration of photoresponsive liquid crystals with the AAA structures. The resonant transmission peak can be tuned by changing the aperture dimensions, leading to continuous color tuning of transmitted light. With the liquid crystals applied to the structure, much higher transmittance can be achieved due to the refractive index matching. More importantly, the transmittance of the color filter can be optically controlled, which could be useful in compact display systems and all-optical information processing. Apart from the guiding devices, practical plasmonic applications also demand frequency control of surface plasmons. For example, surface plasmon based frequency division multiplexing could greatly increase the information processing speed and capacity. A basic requirement here will be the capability to control the frequency shift of the generated signals relative to the pump. In this work, we will show the manipulation of surface plasmon frequency shift through a temporally oscillating metal-insulator-metal waveguide. The frequency shift process of surface plasmons is affected by the waveguide structure and also the amplitude and frequency of the oscillation, and shares the characteristics of Brillouin scattering.

### T16.5 Active plasmonics based on dual-frequency liquid crystals

Yan Jun Liu, Eunice S. P. Leong, Bing Wang, Jing Hua Teng

Friday, February 24, 03.15 PM, Lecture Theatre LT31

Gold nanodisk/hole arrays on a glass substrate were respectively fabricated through electron-beam lithography (EBL) and subsequently overlayed by a dual-frequency liquid crystal (DFLC) layer. For the gold nanodisk array, the localized surface plasmon resonance (LSPR) peak can be actively tuned more than 20 nm using a frequency-dependent electric field; while for the gold nanohole array, the optical transmission can be further enhanced by 11% due to the refractive index matching of the dielectric media on its two sides. By controlling the alignment of the LC molecules, a highly reversible and reproducible tuning behavior for both types of nanostructures is demonstrated.

## 6.16 T17 Physics of Bubbles

This session on "Physics of Bubbles" will be held on Friday, February 24, from 02.00 PM to 03.00 PM. The venue for this session is Seminar Room 03-07. Time allocated for invited talks is 25 min speaking time, plus 5 min questions, and time allocated for contributed talks is 12 min speaking time plus 3 minutes questions.

### T17.1 Cavitation inception with homogeneous nucleation in microfluidic channels

Keita Ando, Ai-Qun Liu, Claus-Dieter Ohl

Friday, February 24, 02.00 PM, Seminar Room 03-07

A microfluidic technique is proposed to measure the ultimate tensile strength of water, which is defined as the largest pressure amplitude for cavitation inception with homogeneous nucleation of vapor bubbles. The small-scale setup is useful for reducing the probability of having heterogeneous nucleation sites, such as stabilized gas bubbles and solid particles, that give rise to significant reductions in the tensile strength. A transparent microchannel is partially filled with clean water to create an air-water interface. An infrared laser pulse is focused into the liquid near the air-water interface; a spherical shock wave results from the expansion of the laser-induced plasma. The shock reflects at the interface, due to acoustic impedance mismatch, as a strong tension wave with high negative pressures. The liquid becomes stretched and eventually ruptures with the nucleation of vapor bubbles. These nucleated bubbles are captured using an optical delay and very short exposure times. Reproducible observations of the bubble nucleation are obtained, supporting our claim of homogeneous bubble nucleation. From comparisons with axisymmetric Euler flow simulation, the threshold of homogeneous cavitation inception for the water is estimated at -60 MPa, which is the largest reported tension for dynamic measurements.

### T17.2 Acoustic cavitation in microfluidics: sonochemistry and sonoluminescence

Tandiono Tandiono, Siew-Wan Ohl, Dave Siak-Wei Ow, Claus-Dieter Ohl

Friday, February 24, 02.15 PM, Seminar Room 03-07

Acoustic cavitation is the creation of empty voids in the form of expansion, contraction, or collapsing of pre-existing gas bubbles (cavitation nuclei) in a liquid with an acoustic wave. During bubble collapse enormous energy concentration is released into the liquid, and the energy is able to trigger non-spontaneous chemical reactions (sonochemistry) and emit light (sonoluminescence). While they have been extensively studied and observed in bulk liquids, there is still a dearth of evidence of these phenomena in microfluidics due to the difficulties in producing strong cavitation in a very confined space. Here, we present a technique to achieve inertial acoustic cavitation by ultrasonic vibration in polydimethylsiloxane (PDMS) based microfluidic devices. The cavitation initiates at gas-liquid interfaces, which are acoustically driven into nonlinear oscillation. The nuclei leading to the inertial cavitation are generated by entrapment of gas pockets at the interfaces. Despite the confined geometry that distorts the bubble sphericity and hence diminishes the energy concentration during collapse, the sonoluminescence and sonochemistry can still be achieved. A well-known oxidation of luminol in a sodium carbonate base solution is used to show the evidence of sonochemistry. The light emission of luminol luminescence and sonoluminescence is detected with a photomultiplier and captured with an intensified CCD camera.

### T17.3 Bubble oscillations near a rigid boundary

Firdaus Prabowo, Claus-Dieter Ohl

Friday, February 24, 02.30 PM, Seminar Room 03-07

Physics of bubble oscillations near boundaries is a well-known problem, however not fully understood. If the boundary is rigid, it has important industrial applications in ultrasonic and megasonic cleaning. We develop a model for small amplitude bubble oscillations near a rigid boundary, taking into account acoustic, thermal and viscous damping effects. We extend the model by calculating wall shear stress on the rigid boundary due to bubble oscillations, under assumptions of potential flow around the bubble matched with approximation of thin boundary layer at the rigid boundary. An analytical solution was found for the problem which allows calculating the wall shear stress for relatively long period of oscillations, hence exposing the existence of steady wall shear stress. The model is applied for simulation of ultrasonic cleaning, in which the bubbles are the cleaning agents. Results suggest that under resonant condition, driving frequency of order $10\hat{6}$ Hz may yield the maximum wall shear stress. This may be one of the reasons of the success of megasonic cleaning in semiconductor industry. The effect of viscosity to the wall shear stress is also investigated since it has two contradictory contributions; it is proportional to the wall shear stress but it also dampens the bubble oscillations which actuate the flow. We found optimum viscosities for the problem using a range of driving frequency of interest.

### T17.4 Vortical flow Generated by Cavitation Bubbles

Fabian Reuter, Silvestre Roberto González Ávila, Claus-Dieter Ohl

Friday, February 24, 02.45 PM, Seminar Room 03-07

The interest on the behaviour of cavitation bubbles raises from their frequent occurrence in technical applications, where they can be unwanted and destructive, as in turbines or ships, or beneficial as in sonochemistry or cleaning applications. So far the dynamics of the bubble and its surrounding fluid is rather well understood during the expansion and shrinkage. However, most bubbles shrink/collapse non spherically, thereby creating a vortex flow. Very little is known of the dynamics of this vortex and its interaction with a nearby boundary. Here, we study the flow field generated after the collapse of a single vapor bubble near to boundary is studied with particle image velocimetry (PIV) technique. Therefore, a single bubble is created close to a rigid boundary by a focussed laser pulse. The liquid is contained in a cuvette filled with water and fluorescent tracer particles. The laser focus position can be adjusted so that the bubble can be created at different distances from the boundary. We implement two high-speed cameras to study the fast bubble dynamics during collapse with 500,000 frames per second while we record the PIV images with up to 40,000 frames per second. Challenges in this study are the fast dynamics with flow speeds up to 100 m/s and the high flow field gradients demanding the use of very small sized articles. Results show markedly different dynamics for different distances of the bubble from the boundary. In particular we find long lived vortical structures travelling both, towards and away from the boundary. They may be important for application in ultrasonic cleaning and mixing.

## 6.17 T18 Metamaterials

This session on "Metamaterials" will be held on Friday, February 24, from 04.00 PM to 05.15 PM. The venue for this session is Lecture Theatre LT31. Time allocated for invited talks is 25 min speaking time, plus 5 min questions, and time allocated for contributed talks is 12 min speaking time plus 3 minutes questions.

### T18.1 Light Control through Transformation Optics: From Invisibility to Imaging and Plasmonic Applications (INVITED)

Baile Zhang

Friday, February 24, 04.00 PM, Lecture Theatre LT31

Transformation optics, as a new powerful strategy of manipulating light or electromagnetic waves, has attracted a lot of interest in the past few years. However, how to implement transformation-based devices at optical frequencies is still a challenging problem, mainly because of the two difficulties of material fabrication—-anisotropy and inhomogeneity, corresponding to nonconformal mapping and conformal mapping respectively. In this talk, we will briefly discuss the strategy to reconcile these two difficulties in different applications, based on nonconformal or conformal mapping.

We will start with the application in invisibility cloaking. The advantages of our recent proposal of utilizing anisotropy while avoiding inhomogeneity will be discussed. Then the extension to subwavelength imaging will also be introduced based on the conformal mapping. Finally, how to apply this strategy in plasmonic applications, such as plasmonic circuits and plasmonic resonators, will be explored with implementable practical models.

### T18.2 Direct laser writing of three dimensional metamaterials (INVITED)

Andrew Bettiol

Friday, February 24, 04.30 PM, Lecture Theatre LT31

The rapid research progress made in recent years in artificially structured sub-wavelength metallic structures, or metamaterials, has been driven by the desire to make materials that possess electromagnetic properties that cannot be found in nature. The ability to directly control the effective permittivity ($\varepsilon$) and permeability ($\mu$) of these materials through top down fabrication technology has opened up many potential applications such as negative refractive index, optical magnetism, slow light, cloaking, superlensing, broadband polarizers and sensing. The majority of the metamaterials that have been demonstrated thus far have been fabricated using planar lithographic techniques such as electron beam lithography or UV lithography. In an attempt to increase the interaction length between the impinging electromagnetic radiation and the metamaterial, research has recently moved towards extending fabrication technologies to the third dimension.

This talk will discuss the use of three dimensional direct laser writing utilizing two photon polymerization (TPP) for fabricating metamaterials. TPP is particularly appealing as it is the only technique that allows for arbitrary three dimensional control over the fabrication process.The technique utilizes nonlinear optical absorption of a tightly focused pulsed laser beam to selectively crosslink a small volume inside a polymer. By moving the focal point relative to the sample in all three dimensions, arbitrary three dimensional nanostructures can be fabricated.

### T18.3 Generalized Phononic Networks: Controlling Complexity through Simplicity

Cheongyang Koh, Edwin Thomas

Friday, February 24, 05.00 PM, Lecture Theatre LT31

The manipulation and control of phonons is extremely important from both a fundamental scientific and applied technological standpoint, providing applications ranging from sound insulation to heat management. Phononic crystals and metamaterials are artificially structured materials (at certain length scales) that provide promise in controlling the propagation of phonons in solids. However, the vector nature of the phonon makes the development of a governing framework with which to guide the design of these phononic metamaterials complicated and no coherent framework currently exists for the design of phononic structures. In this work, we utilize a combination of global symmetry principles, adopted from group theory and the theory of representations, together with conservation principles and broken symmetry concepts to formulate our generalized design framework. In particular, we are able to explain the choice of a particular physical topography for a desired phononic propagation behavior in a coherent fashion. In addition, we show how to explicitly control the dispersion relations of a phononic metamaterial in order to obtain a desired final band structure. Demonstrations range from a new polychromatic phononic metamaterial which possesses multiple complete in-plane spectral gaps totaling over 100% in normalized gap size to a phononic metamaterial which exhibits a single complete in-plane spectral gap of 102% and a complete spectral gap of 88%, both significant advancements over the state of the art. We show that only a few governing principles are required to design the desirable band dispersion relations of such phononic metamaterials. The generality of our framework allows extension to other vector and scalar waves, such as photonic, plasmonic and magnonic structures and provides a promising route forward to the development of integrated structured material platforms that allow for the rational manipulation and interactions of phonons with other waves, such as phonons and spin waves.

## 6.18 T19 Nanoactuators

This session on "Nanoactuators" will be held on Friday, February 24, from 04.00 PM to 05.00 PM. The venue for this session is Seminar Room 03-07. Time allocated for invited talks is 25 min speaking time, plus 5 min questions, and time allocated for contributed talks is 12 min speaking time plus 3 minutes questions.

### T19.1 Molecular motors: from biophysics to motor-based nanotechnology (INVITED)

Zhisong Wang

Friday, February 24, 04.00 PM, Seminar Room 03-07

Miniaturized motor systems made of individual biomolecules are abundant in cells of our human body. These molecular motors are indispensable to vital biological processes such as intracellular transport, cell division, signal transduction, and cell motility. The biophysical study of cellular motors has inspired a multidisciplinary thrust to develop artificial mimics (often called nanomotors). Indeed, molecular motors or nanomotors may be regarded as the nanoscale counterpart of heat engines that had fueled the Great Industrial Revolution; and a motor-based nanotechnology may be envisioned. In this talk, I shall present a personal overview of the emerging interdisciplinary field of molecular motors science and technology. I shall also discuss some latest research of our Molecular Motors Lab at Physics@ NUS.

### T19.2 Carbon Nanotubes Based Laser-Induced Micro-Actuators and Scaffolds for Assembly of Nanomaterials (INVITED)

Chornghaur Sow

Friday, February 24, 04.30 PM, Seminar Room 03-07

We have developed a simple focused laser pruning technique to fabricate two and three-dimensional (3D) microstructures made of aligned array of multi-walled Carbon Nanotubes (MWCNTs). Using this focused laser beam nanofabrication technique, we created a wide variety of 3D microstructures for the selective assembly of nanoparticles (ZnO), quantum dots (QDs) and even recrystallized CuSO4 microcrystal from solution en route to unique functional hybrid nanomaterial systems. Details of the fabrications and characterization of the hybrid nanomaterial and some of its unique properties will be presented. During the assembly of nanoparticles (NPs) onto the MWCNT, the aligned array of MWCNTs scaffold was found to be effective NanoSieve that could sort out NPs with a very small size difference (  1nm). In this case, a droplet of solution comprising NPs of different sizes was placed on aligned array of MWCNTs. During the deposition, the smaller NPs were found to assemble deeper into the MWCNTs. These NPs could be revealed after part of the MWCNTs was removed by laser pruning. Fluorescence microscopy showed multi-colored MWCNT microstructures due to preferential decoration of these NPs with difference sizes. The characteristics of the size dependent decoration of NPs onto the MWCNTs forest will be discussed. In addition, the same focused laser beam was able to cause mechanical actuation of MWCNTs microstructures after they are fabricated. Such behavior was exploited in creating simple micro-actuators comprising the microstructures made of MWCNTs. This technique is convenient and effective, and has potential applications in the fabrication of unique devices.

## 6.19 T20 Organic Electronics

This session on "Organic Electronics" will be held on Friday, February 24, from 04.00 PM to 05.00 PM. The venue for this session is Seminar Room 03-04. Time allocated for invited talks is 25 min speaking time, plus 5 min questions, and time allocated for contributed talks is 12 min speaking time plus 3 minutes questions.

### T20.1 Nonvolatile memory concepts from organic ferroelectrics (INVITED)

Damar Yoga Kusuma, Pooi See Lee

Friday, February 24, 04.00 PM, Seminar Room 03-04

With the advancement of organic electronics, various types of organic memories which can store and retrieve data are becoming critically important in multiplexing plastic integrated circuits. Electrically bistable switching behaviour has been observed in many organic semiconductors or composite materials which can offer a low-cost, flexible and solution processable printable electronics. The attractive features of ferroelectric memory include high ON/OFF current ratio, scalable cell size, low power consumption, intrinsic stability of the ferroelectric polarization and the potentially low fabrication costs resulting from a bottom-up approach. While memory devices based on inorganic ferroelectric have been developed and commercially available, it is not the case for organic ferroelectric memories. Several challenges, including slow switching kinetics, shift of threshold voltage, as well as relatively short data retention hinder further developments and commercialization.

In this paper, several approaches are presented to address the challenges. In this regard, a small amount of nanoparticles was blended into ferroelectric polymer PVDF-TrFE resulting in more than 3 orders of magnitudes enhancement on its switching kinetics. The enhancement is discussed in terms of promoted heterogeneous nucleation within the ferroelectric domains with the nanoparticles as nucleation centers. In addressing the threshold voltage shift, a study of ferroelectric field-effect transistor (Fe-FET) and the interfaced with organosilane self-assembled monolayer (SAM) was performed. Employing the polar dipole nature of SAM molecules, control over threshold voltage shift can be realized. Lastly, we demonstrate conductance bi-stability via the ferroelectric polarization switching in two terminals ferroelectric tunnel junction device. The resulting robust and uniform few monolayer film allows the fabrication and characterization of non-localized tunnel junction memory device.

### T20.2 Control of Defects and Dopants in Single Crystals of Organic Semiconductors (INVITED)

Hui Jiang, Ke Jie Tan, Keke Zhang, Irvine Hong Huamin, Christian Kloc

Friday, February 24, 04.30 PM, Seminar Room 03-04

The band structure and the crystalline structure of organic semiconductors are determined by the chemical formula of molecules arranged into a single crystal. The intrinsic properties resulting from that composition and structure are not straightforwardly available from measurements. The measured electrical and optical properties of organic semiconductors are shaped by defects, dopants and contaminants. Therefore, the structure – property relations, explored for individual molecular semiconductor, are mostly extrinsic values and only partially useful for design of new, more efficient organic semiconductors. Thus, separation of external properties from intrinsic properties and generalization of those onto large families of organic compounds would require purification and growth of high quality crystals, as well as development of impurities and defects characterization methods suitable for organic semiconductors. Rubrene is an ideal candidate for studies of structure-property relation since rubrene crystallizes readily and shows relative high mobility of charge carriers. Single crystals were grown by a vapor transport method and field effect transistors were prepared. The impurities formed during the synthesis, as well as formed during rubrene reaction with ambient atmosphere were detected and separated. We correlate the appearance of photoluminescence peaks and rubrene transport properties with oxygen-related defects and associate the observed extrinsic properties with crystal growth environment. We conclude that the high mobility value of rubrene is not an intrinsic property but is the results of peculiar oxidation mechanism of rubrene surface. The measured properties of organic semiconductors reveal an interaction between defects, dopants and contaminants, especially those located on surfaces and interfaces. Therefore, the current effort to achieve effective transport in organic semiconductors by tailoring only the chemical formula of molecules needs to be revised.

## 7 Committees

### Program Committee

KOH Wee Shing, A*STAR Institute of High Performance Computing

KWEK Leong-Chuan, CQT / NIE

SOW Chorng Haur, Physics Department, NUS

ZHANG Qing, Division of Microelectronics, NTU

Christian KURTSIEFER (chair), CQT / Physics Departement, NUS

### Organizing Committee

Markus BADEN, CQT

CHANG Chui Theng, CQT

Andreas DEWANTO, Faculty of Science, NUS

LIM Kim Yong, Faculty of Science, NUS

Alexander LING, CQT / Physics Departement, NUS

Evon TAN, CQT

## Author List